





# Orphan nuclear receptor COUP-TFII enhances myofibroblast glycolysis leading to kidney fibrosis

Li Li<sup>1,2,\*</sup> , Pierre Galichon<sup>1,2</sup>, Xiaoyan Xiao<sup>1</sup>, Ana C Figueroa-Ramirez<sup>1</sup>, Diana Tamayo<sup>1</sup>, Jake J-K Lee<sup>3</sup>, Marian Kalocsay<sup>4,5</sup> , David Gonzalez-Sanchez<sup>1</sup>, Maria S Chancay<sup>1</sup>, Kyle W McCracken<sup>1,2</sup>, Nathan N Lee<sup>1</sup>, Takaharu Ichimura<sup>1,2</sup>, Yutaro Mori<sup>1</sup>, M Todd Valerius<sup>1,2,6</sup> , Julia Wilflingseder<sup>1</sup>, Dario R Lemos<sup>1,2</sup>, Elazer R Edelman<sup>2,7,8</sup> & Joseph V Bonventre<sup>1,2,4,6,\*\*</sup> 

## Abstract

Recent studies demonstrate that metabolic disturbance, such as augmented glycolysis, contributes to fibrosis. The molecular regulation of this metabolic perturbation in fibrosis, however, has been elusive. COUP-TFII (also known as NR2F2) is an important regulator of glucose and lipid metabolism. Its contribution to organ fibrosis is undefined. Here, we found increased COUP-TFII expression in myofibroblasts in human fibrotic kidneys, lungs, kidney organoids, and mouse kidneys after injury. Genetic ablation of COUP-TFII in mice resulted in attenuation of injury-induced kidney fibrosis. A non-biased proteomic study revealed the suppression of fatty acid oxidation and the enhancement of glycolysis pathways in COUP-TFII overexpressing fibroblasts. Overexpression of COUP-TFII in fibroblasts also induced production of alpha-smooth muscle actin ( $\alpha$ SMA) and collagen 1. Knockout of COUP-TFII decreased glycolysis and collagen 1 levels in fibroblasts. Chip-qPCR revealed the binding of COUP-TFII on the promoter of PGC1 $\alpha$ . Overexpression of COUP-TFII reduced the cellular level of PGC1 $\alpha$ . Targeting COUP-TFII serves as a novel treatment approach for mitigating fibrosis in chronic kidney disease and potentially fibrosis in other organs.

**Keywords** acute kidney injury; COUP-TFII; fibrosis; glycolysis; TGF $\beta$

**Subject Categories** Metabolism; Molecular Biology of Disease

**DOI** 10.15252/embr.202051169 | Received 24 June 2020 | Revised 28 March 2021 | Accepted 1 April 2021 | Published online 25 May 2021

**EMBO Reports (2021) 22: e51169**

## Introduction

Kidney fibrosis is a pathologic hallmark of chronic kidney disease (CKD), which affects ~10% of the world's adult population (Jha *et al*, 2013; Romagnani *et al*, 2017). The progressive deposition and expansion of the fibrotic matrix in kidney parenchyma ultimately lead to kidney failure (Bonventre & Yang, 2011; Rockey *et al*, 2015). Fibrosis also plays an important role in other chronic diseases, such as liver cirrhosis, idiopathic pulmonary fibrosis, and scleroderma (Wynn & Ramalingam, 2012). The global burden of fibrotic disease is high, with an estimated prevalence rate of one in four people (Zhao *et al*, 2019, 2020). Currently, there is no cure for fibrosis, highlighting the need for a new strategy and a better understanding of the molecular mechanisms underlying fibrosis. It is generally accepted that myofibroblasts are major cellular contributors to fibrotic disease (Tomasek *et al*, 2002; Bonventre & Yang, 2011; Duffield *et al*, 2013; Duffield, 2014). Myofibroblasts express alpha-smooth muscle actin ( $\alpha$ SMA) and contract, migrate, and produce excessive extracellular matrix (ECM) (Klingberg *et al*, 2013). Comprehensive genetic fate-mapping studies in rodents indicate that kidney resident *Foxd1* expressing pericytes/perivascular fibroblasts/mesenchymal stem cell-like stromal cells are the main source of myofibroblasts after kidney injury (Humphreys *et al*, 2008; Lin *et al*, 2008; Picard *et al*, 2008; Humphreys *et al*, 2010; Kobayashi *et al*, 2014; Falke *et al*, 2015; Kramann *et al*, 2015).

Recently, an emerging body of evidence has demonstrated the link between metabolic dysregulation and fibrosis (Xie *et al*, 2015; Lan *et al*, 2016; Hou & Syn, 2018; Zank *et al*, 2018). Genome-wide transcriptome profiling revealed inflammation and metabolism as the top dysregulated pathways in fibrotic human kidneys (Kang *et al*, 2015). A similar analysis of human skin fibrosis identified

1 Division of Renal Medicine, Brigham and Women's Hospital, Boston, MA, USA

2 Department of Medicine, Harvard Medical School, Boston, MA, USA

3 Department of Biomedical Informatics, Harvard Medical School, Boston, MA, USA

4 Laboratory of Systems Pharmacology, Harvard Medical School, Boston, MA, USA

5 Department of Systems Biology, Harvard Medical School, Boston, MA, USA

6 Harvard Stem Cell Institute, Cambridge, MA, USA

7 Cardiovascular Division, Brigham and Women's Hospital, Boston, MA, USA

8 Institute for Medical Engineering and Science, Massachusetts Institute of Technology, Cambridge, MA, USA

\*Corresponding author. Tel: +1 801 550 5529; E-mail: lli29@bwh.harvard.edu

\*\*Corresponding author. Tel: +1 617 525 5966; E-mail: jbonventre@bwh.harvard.edu

perturbations of fatty acid oxidation (FAO) and glycolysis pathways (Zhao *et al*, 2019). Inhibition of glycolysis or restoring FAO by genetic or pharmacological methods mitigated fibrosis in various animal models (Kang *et al*, 2015; Tran *et al*, 2016; Ding *et al*, 2017; Han *et al*, 2017; Zhao *et al*, 2019, 2020). Despite these preliminary findings, the exact mechanisms that regulate metabolic dysregulation, especially in myofibroblasts, remain largely unknown.

Chicken ovalbumin upstream promoter-transcription factor II (COUP-TFII, also known as *NR2F2*) is an orphan member of the nuclear receptor family with unknown endogenous ligands (Pereira *et al*, 1999). Since COUP-TFII has been reported to regulate metabolic functions (Li *et al*, 2009; Planchais *et al*, 2015; Ashraf *et al*, 2019), we evaluated whether it played an important role in fibrosis. Downstream proteins under COUP-TFII control tend to be involved in energy production, anabolic pathways, and cell cycle progression, all of which impact cell proliferation (Chen *et al*, 2012; Planchais *et al*, 2015; Wu *et al*, 2015). Up-regulation of COUP-TFII in numerous cancers, such as colon (Bao *et al*, 2014), pancreas (Polvani *et al*, 2014), prostate (Qin *et al*, 2013), and renal cell carcinoma (Fang *et al*, 2020), further supports the role of COUP-TFII in promoting cell proliferation. We hypothesized that COUP-TFII contributed to organ fibrosis via a regulatory role in the metabolism of the myofibroblast.

In this study, we demonstrate that COUP-TFII facilitates the shift of myofibroblast metabolism toward enhanced glycolysis and generation of profibrotic mediators. Increased COUP-TFII expression co-localized with  $\alpha$ SMA expression in stromal cells of fibrotic human kidneys, lungs, kidney organoids, and fibrotic mouse kidneys after injury. Ablation of COUP-TFII in adult mice attenuated injury-induced kidney fibrosis. Our findings demonstrate a previously unrecognized role of COUP-TFII on regulating myofibroblast differentiation and highlight COUP-TFII as a relevant therapeutic target to prevent organ fibrosis after injury.

## Results

### COUP-TFII expression is increased in myofibroblasts in human fibrotic diseases and human kidney organoids

We interrogated previously published, human CKD microarray datasets and found a significant increase in COUP-TFII mRNA levels

(1.9-fold) in renal biopsy tissues of 53 patients with CKD (GSE66494; Fig 1A) (Nakagawa *et al*, 2015). In another large cohort ( $n = 95$ ) of microdissected human kidney samples from diabetic or hypertensive CKD subjects with pathology-defined fibrosis, microarray transcription profiling also revealed a significant up-regulation of COUP-TFII by analysis of total kidney mRNA levels (1.33-fold) (Kang *et al*, 2015). Results from these two independent cohorts of patients suggest an association between COUP-TFII mRNA expression and CKD in humans. We confirmed COUP-TFII protein expression and localization by immunofluorescent staining of normal and diseased human kidneys. In control “healthy” kidney tissues, which were obtained from the non-tumor portions of total nephrectomy samples from patients with renal cell carcinoma, we found little scattered COUP-TFII expression (Fig 1B). In the setting of kidney injury (patients with either acute thrombotic microangiopathy [TMA] or chronic diabetic nephropathy [DN]), however, the number of COUP-TFII-positive cells was significantly increased (Fig 1B). The majority of these cells were localized in the interstitial region and co-localized with expanded  $\alpha$ SMA-positive areas of fibrosis (Fig 1B). Similar results were also identified in human fibrotic lungs from two patients with idiopathic pulmonary fibrosis (IPF; Fig 1C).

We also examined COUP-TFII expression in human kidney organoids generated by directed differentiation of human pluripotent stem cells (Morizane *et al*, 2015). Human kidney organoids provide advantages of 3D nephron structures with multiple human kidney cell types and a rich stroma. Fibrosis of human kidney organoids was induced by incubation with IL-1 $\beta$  for 96 h as previously reported (Lemos *et al*, 2018). As shown in Fig 1D, COUP-TFII expression significantly increased in IL-1 $\beta$ -treated organoids compared with control organoids treated with vehicle. Most COUP-TFII-positive cells were located in the interstitial region and co-localized with  $\alpha$ SMA, as observed in the kidneys of human subjects with CKD. In addition to IL-1 $\beta$ , we also treated organoids with PDGF, TGF $\beta$ 1, or cobalt chloride (CoCl<sub>2</sub>, which induces hypoxia-inducible factor [HIF] signaling, mimicking the response to hypoxia) in an attempt to screen for the upstream activators of COUP-TFII. As shown in Fig 1E, COUP-TFII expression increased significantly in organoids treated with TGF $\beta$ 1 and cobalt chloride, but not PDGF. Together, these results indicate an association of increased COUP-TFII expression with fibrosis in human kidney tissue. The potential link to fibrosis prompted us to investigate the spatial and temporal

**Figure 1. COUP-TFII expression is increased in human fibrotic kidneys and lungs, and human kidney organoids.**

- A COUP-TFII mRNA levels in human kidney tissues of control ( $n = 8$ ) and CKD ( $n = 53$ ) subjects from GSE66494. \*\*\* $P < 0.001$  by *t*-test.
- B COUP-TFII expression (green) is increased in human kidneys from patients with thrombotic microangiopathy (TMA) and diabetic nephropathy (DN;  $n = 2$ ). Quantification of mean of 7–10 confocal images per patient at 400 $\times$  hpf. \*\*\*\* $P < 0.0001$  by one-way ANOVA; mean  $\pm$  SD. The majority of these cells were localized in the interstitial region. More than 50% COUP-TFII (+) cells (green) are co-localized with expanded  $\alpha$ SMA-positive (red) areas of fibrosis. Pearson correlation coefficient (PCC) = 0.56  $\pm$  0.1 for patient#1 and 0.65  $\pm$  0.13 for patient#2.
- C COUP-TFII expression (green) is increased in lungs from patients with IPF ( $n = 2$ ) by immunofluorescence. Quantification of mean of 7–10 confocal images per patient at 400 $\times$  hpf. \*\* $P < 0.01$ ; \*\*\*\* $P < 0.0001$  by one-way ANOVA, mean  $\pm$  SD.
- D Human kidney organoids were treated with IL-1 $\beta$  (10 ng/ml) for 96 h. Immunofluorescence reveals significantly increased COUP-TFII (green) and  $\alpha$ SMA (red) expression in IL-1 $\beta$ -treated organoids, compared with non-treated organoids. Quantification by confocal micrographs in 200 $\times$  hpf. \*\* $P < 0.01$ ; \*\*\* $P < 0.001$  by *t*-test; mean  $\pm$  SD.
- E COUP-TFII expression increased significantly in organoids treated with TGF $\beta$ 1 (10 ng/ml), cobalt chloride (100  $\mu$ M), IL-1 $\beta$  (10 ng/ml), but not PDGF (50 ng/ml). Quantification by confocal micrographs in 400 $\times$  hpf. \* $P < 0.05$ ; \*\* $P < 0.01$ ; \*\*\*\* $P < 0.0001$  by one-way ANOVA, mean  $\pm$  SD. The higher magnification of the insert from IL-1 $\beta$  showed co-localization of COUP-TFII (green) and  $\alpha$ SMA (red) staining.

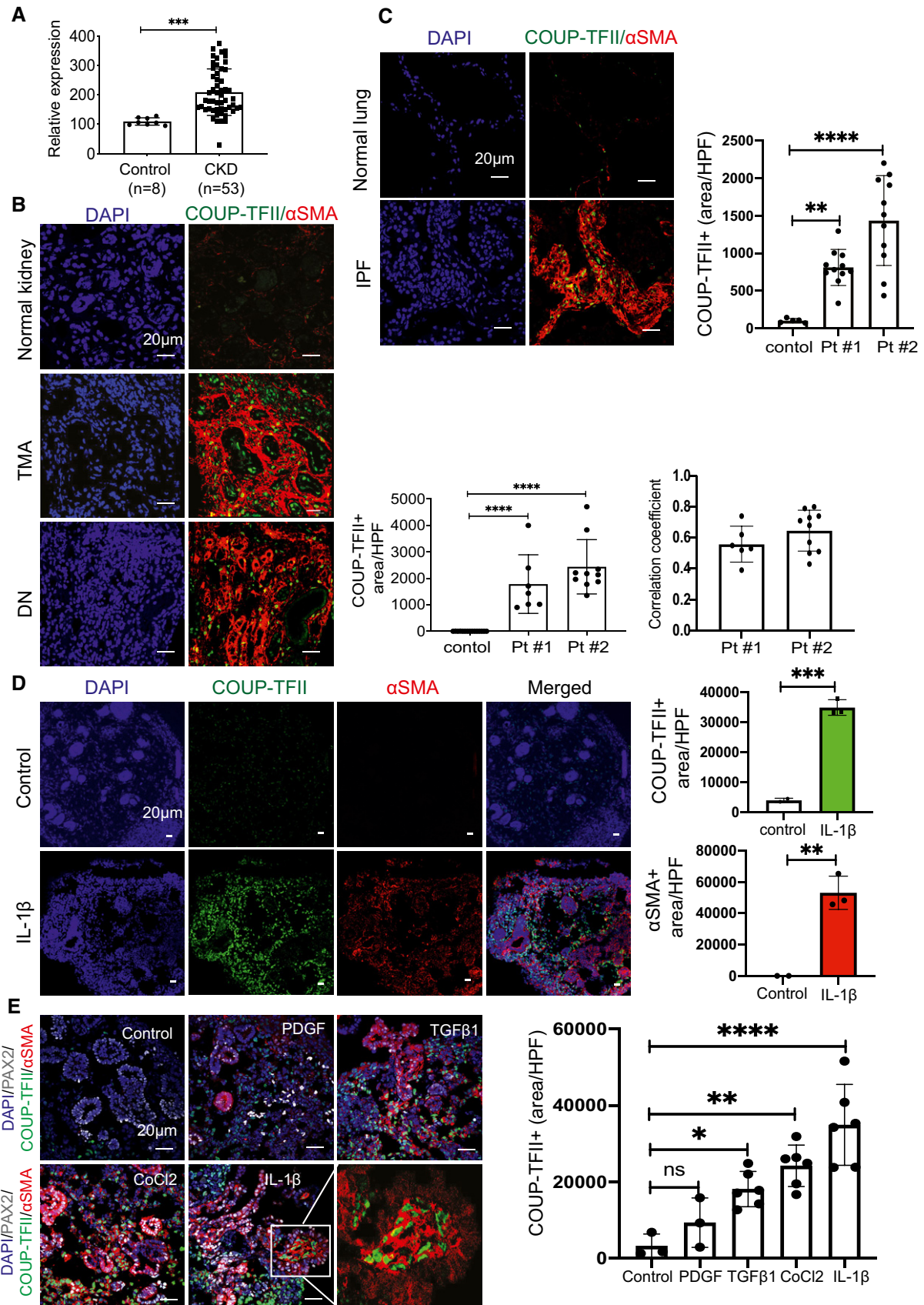


Figure 1.

expression, and mechanistic implications of COUP-TFII in non-injured and injured kidneys in adult mice.

### COUP-TFII protein is expressed in stromal cells in non-injured and injured mouse kidneys

In healthy adult mouse kidneys, a few scattered COUP-TFII-positive cells were present within the interstitium. The majority of COUP-TFII-positive cells expressed PDGFR $\beta$ , a pericyte/fibroblast marker. COUP-TFII was not observed in endothelial cells marked by CD31 (Fig 2A).

To further assess the developmental origin of COUP-TFII<sup>+</sup> cells, we crossed *Foxd1*-Cre driver mice (Humphreys *et al*, 2010) to tdTomato reporter mice (Madisen *et al*, 2010) to genetically label the *Foxd1*-derived stromal cells (Fig 2B). The majority of COUP-TFII protein-expressing cells (green) were also tdTomato-labeled *Foxd1*-derived stromal cells (red; Fig 2C), demonstrating that COUP-TFII<sup>+</sup> cells in non-injured mice derive from the *Foxd1* population. Analysis of an available single-cell RNA sequencing database (<http://humphreyslab.com/SingleCell/>) (Wilson *et al*, 2019; Wu *et al*, 2019) confirmed that COUP-TFII RNA was most enriched in pericyte/fibroblast cells in injured kidneys, both in human (diabetic kidney; Fig 2D top) and mouse (UUO day 14; Fig 2D bottom). Thus, the majority of COUP-TFII<sup>+</sup> cells are kidney stromal cells, both in non-injured and injured kidneys.

### COUP-TFII expression is increased during the development of kidney fibrosis in various kidney injury models in mice

COUP-TFII expression was significantly increased and co-localized in  $\alpha$ SMA<sup>+</sup> cells within fibrotic regions in the injured kidney in two mouse kidney injury models: unilateral ureteral obstruction (UUO) and unilateral ischemia-reperfusion injury (UIRI; Fig 3A). To further characterize the spatial and temporal expression kinetics of COUP-TFII, we focused on the UUO model since it more reliably induces fibrosis in a short time frame. As shown in Fig 3B, COUP-TFII expression was up-regulated as early as day 2 after injury, which is well before up-regulation of  $\alpha$ SMA and any histologic evidence of fibrosis was evident. We further demonstrated that the increased COUP-TFII expression is distinct from the inflammatory infiltrate that accompanies injury and fibrosis, as it does not overlap with markers of T lymphocytes (CD3), neutrophils (LyG6), or macrophages (F4/80; Fig 3C). Thus, we conclude that COUP-TFII is up-regulated specifically within the stromal compartment following kidney injury, and it precedes the expression of fibrotic markers, compatible with a potential causative role in the pathophysiology of fibrosis.

Genetic lineage tracing analysis demonstrated that Gli1 marks perivascular mesenchymal stem cells-like cells, which are proposed to contribute to organ fibrosis (Kramann *et al*, 2015). We evaluated

whether COUP-TFII<sup>+</sup> cells and Gli1<sup>+</sup> cells represent the same or closely related populations. We used the *Gli1*-CreERT2 line crossed with tdTomato reporter mice and induced genetic labeling 10 days prior to UUO injury (Fig 3D). Kidney tissues were collected at day 10 after UUO and stained for COUP-TFII expression. As expected, *Gli1*-derived cells expanded in number and acquired  $\alpha$ SMA expressing by 10 days after UUO (Fig 3E). Co-staining revealed that COUP-TFII expression was indeed found in nearly all of Gli1-tdTomato<sup>+</sup> cells; however, there were also a large number of COUP-TFII<sup>+</sup> cells that were distinct from the Gli1 lineage (Fig 3E). Although some of these cells could result from incomplete labeling with the inducible *Gli1*-Cre, there was also a noticeable difference in the spatial distribution between the COUP-TFII<sup>+</sup>/tdTomato<sup>-</sup> and COUP-TFII<sup>+</sup>/tdTomato<sup>+</sup> populations. Interestingly, while COUP-TFII<sup>+</sup> cells were found throughout both the cortex and medulla, co-localizing in  $\alpha$ SMA<sup>+</sup> cells in both regions, the Gli1-tdTomato<sup>+</sup> cells were largely restricted to the outer medullary region (Fig 3F). This is consistent with the previous observations (Kramann *et al*, 2015) that *Gli1*-tdTomato<sup>+</sup> cells represented only a small fraction of the total PDGFR $\beta$ <sup>+</sup> population. Gli1 cells were enriched in the outer medulla with much less expression in pericytes and perivascular fibroblasts of the cortex (Kramann *et al*, 2015; Humphreys, 2018). As fibrosis is present both in cortex and outer medulla in the UUO model, our data suggest that COUP-TFII functions more generally in regulating pericyte to myofibroblast differentiation, irrespective of the anatomic compartments.

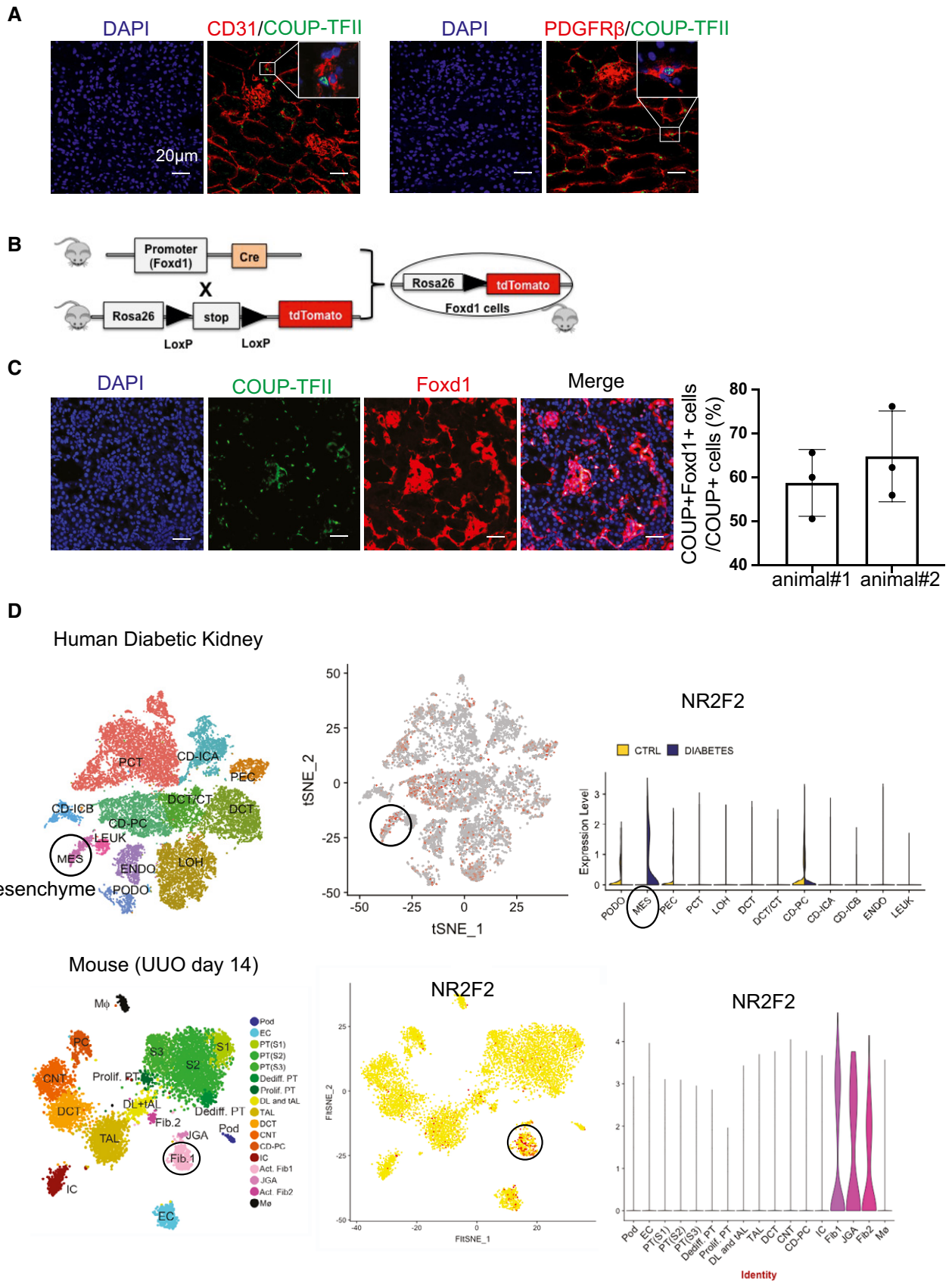
### Ablation of COUP-TFII in adult mice attenuates injury-induced kidney fibrosis

Since global knockout of COUP-TFII in mice confers embryonic arrest at E10 due to defective angiogenesis and cardiac development (Pereira *et al*, 1999), we used a tamoxifen-inducible Cre-loxP system to knockout COUP-TFII in adult mice. We generated COUP-TFII<sup>fllox/+</sup>; Rosa26<sup>CreERT2/+</sup> (*F/+*; *Cre/+*) and COUP-TFII<sup>fllox/fllox</sup>; Rosa26<sup>CreERT2/+</sup> (*F/F*; *Cre/+*) mice. COUP-TFII expression was maintained in these mice without tamoxifen (TAM). Three injections of TAM activated *Cre* recombinase and generated COUP-TFII heterozygous (+/−) and homozygous (−/−) knockout mice. Ten days after TAM injection, mice were subjected to UUO and euthanized 7 days after UUO (Fig 4A). There was no identifiable phenotypic difference between WT and knockout mice without injury.

We first examined the efficacy of COUP-TFII ablation. A *LacZ* knock-in allele was inserted into the genomic COUP-TFII locus after the second *LoxP* site (Takamoto *et al*, 2005). Treatment with *Cre* recombinase resulted in COUP-TFII deletion and the expression of the *LacZ* reporter. Using this *LacZ* reporter, we were able to trace the COUP-TFII lineage following deletion. As shown in Fig 4B, expression of  $\beta$ -galactosidase ( $\beta$ -Gal) increased after TAM injection

**Figure 2. COUP-TFII protein is expressed in pericytes/fibroblasts, both in non-injured and injured mouse kidneys.**

- A COUP-TFII<sup>+</sup> cells (green) express pericyte/fibroblast marker (PDGFR $\beta$ ) but not the endothelial cell marker (CD31).
- B Strategy of genetically labeling *Foxd1*-derived stromal cells in non-injured mouse kidney.
- C Most COUP-TFII<sup>+</sup> cells (green) were also positive for *Foxd1* (tdTomato-labeled as red) in the non-injured mice kidney (*n* = 2). Quantification by confocal micrographs in 400 $\times$  hpf.
- D COUP-TFII was enriched most in pericytes/fibroblasts in injured kidney, both in the human (Diabetic kidneys, (D) top) and mouse model (UUO day 14, (D) bottom) as analyzed from single-cell sequencing database (<http://humphreyslab.com/SingleCell/>).



in UUO kidneys of heterozygous mice with Cre allele, but not in the control mice with a flox allele but without Cre allele (WT), indicating the specificity of  $\beta$ -Gal staining in the *Cre-LoxP* system. Expression of COUP-TFII decreased after TAM injection in heterozygous (+/−) mice. Ten days after TAM injection,  $\beta$ -Gal expression colocalized with COUP-TFII expression in both contralateral and UUO kidneys, consistent with the deletion of one allele of COUP-TFII (Fig 4C). Both  $\beta$ -Gal expression and COUP-TFII expression increased in UUO kidney compared with contralateral non-injured kidney (Fig 4C).  $\beta$ -Gal staining demonstrated that this population remained stable following TAM injection, indicating that COUP-TFII deletion does not impact the survival or proliferation of these cells at baseline.

Next, we examined the effect of COUP-TFII ablation on injury-induced kidney fibrosis (UUO model) using knockout (KO, −/−) mice. As shown in Fig 4D, COUP-TFII-positive cells decreased significantly in a KO (−/−) mice after UUO compared with WT kidneys, indicating successful knockout of COUP-TFII. Associated with much less COUP-TFII expression,  $\alpha$ SMA and collagen 1 expression was significantly decreased in KO compared with WT at 7 days after UUO. Histological evaluation demonstrated less kidney fibrosis in KO compared with WT by Masson Trichrome (Fig 4D). These data demonstrated that ablation of COUP-TFII in adult mice attenuates injury-induced kidney fibrosis.

### COUP-TFII regulates myofibroblast differentiation *in vitro* through augmented glycolysis

In order to dissect the mechanistic role of COUP-TFII in myofibroblast differentiation, which leads to fibrosis, we generated COUP-TFII loss- and gain-of-function cell lines using CRISPR-Cas9 (clustered regularly interspaced short palindromic repeats [CRISPR]–CRISPR-associated protein 9 [Cas9]) and an inducible lentiviral construct, respectively, in the pericyte-like cell line C3H/10T1/2. C3H/10T1/2 is a mouse mesenchymal cell that has been used in studies related to pericyte biology and cell fate determination *in vitro* (Pinney & Emerson, 1989; Kale *et al.*, 2005; Pecot *et al.*, 2013). Naïve C3H/10T1/2 cells (WT) showed basal expression of COUP-TFII, which we were able to successfully modulate using the knockout (KO) or overexpression (OE) systems (Fig 5A). Neither KO nor OE affected cell viability (Fig 5B), although a decreased proliferation rate in KO cells and increased proliferation rate in OE cells were observed compared with naïve (WT) cells (Fig 5C). Treatment of C3H/10T1/2 cells with TGF $\beta$ 1 induces myofibroblast differentiation with up-regulation of  $\alpha$ SMA (Fig 5D). Interestingly, OE cells, in the absence of TGF $\beta$ 1 stimulation, displayed an elongated fibroblast shape,

similar to WT cells treated with TGF $\beta$ 1 (Fig 5D). There was increased expression of  $\alpha$ SMA and collagen 1 in COUP-TFII OE cells even in the absence of TGF $\beta$ 1 stimulation (Fig 5D and E), while their expression was significantly diminished in the KO cells. Collectively, these data further support a profibrotic function for COUP-TFII in pericyte/fibroblast-like cells.

To further interrogate the molecular mechanisms by which COUP-TFII regulates myofibroblast differentiation, we evaluated the proteome of WT and OE cells that were differentiated with TGF $\beta$ 1. This non-biased approach unequivocally implicated cellular metabolic pathways as predominant direct or indirect targets of COUP-TFII. Gene set enrichment analysis (GSEA) highlighted that the most significantly down-regulated proteins in COUP-TFII-OE cells were enriched in mitochondrial electron transport chain and fatty acid oxidation (FAO) pathways (Fig 6A), which are involved in oxidative metabolism. Conversely, the top up-regulated pathways in COUP-TFII-OE cells were associated with both extracellular matrix, including collagen fiber organization, cadherin binding and actin cytoskeleton, and glycolysis pathways (Fig 6A and B). Taken together, these data support a model in which COUP-TFII enhances glycolysis and suppresses FAO, which may lead to increased extracellular matrix production and fibrosis.

Indeed, we found that COUP-TFII overexpression significantly increased lactate production with or without TGF $\beta$ 1 stimulation compared with WT cells (Fig 6C), consistent with augmented glycolysis in these cells. Furthermore, we performed a glycolysis stress test using the Seahorse X24 extracellular flux analyzer. All three types of cells (WT, OE, and KO), treated with or without TGF $\beta$ 1, were incubated in the glycolysis stress test medium (no glucose and pyruvate). Then, the cells received serial exposures to glucose, oligomycin, and 2-deoxyglucose (2-DG; a glucose analog that inhibits glycolysis through competitive binding to hexokinase2 (HK2), the first enzyme in the glycolytic pathway; Fig 6D). The extracellular acidification rate (ECAR) at baseline, the rate of glycolysis, glycolytic capacity, and glycolytic reserve were determined. Without TGF $\beta$ 1 treatment, COUP-TFII overexpression did not change the baseline ECAR, the rate of glycolysis, glycolytic capacity, or glycolytic reserve. Interestingly, COUP-TFII knockout significantly decreased glycolytic capacity and reserve compared with WT (Fig 6E). TGF $\beta$ 1 significantly increased baseline ECAR, glycolysis, glycolytic capacity, and reserve in WT cells (Fig 6E). This effect of TGF $\beta$ 1 on ECAR was significantly enhanced by COUP-TFII overexpression and reduced by COUP-TFII knockout (Fig 6E). Of note, unlike the lactate assay, COUP-TFII OE cells did not increase glycolysis without TGF $\beta$ 1 stimulation (Fig 6E). This was likely due to the fact that the base medium used in Seahorse experiments did not

### Figure 3. COUP-TFII expression is increased in the injured mouse kidneys during the development of kidney fibrosis.

- A COUP-TFII expression is significantly increased and co-localized with  $\alpha$ SMA<sup>+</sup> cells at day 10 of UUO and day 14 of UIRI in mice ( $n = 3$  animals per group). Quantification of mean of 8–10 confocal images per animal at 200 $\times$  hpf. \* $P < 0.05$  \*\* $P < 0.01$  by paired *t*-test; mean  $\pm$  SD. CTL: contralateral kidney.
- B In a time course of UUO, COUP-TFII expression increased as early as day 2 and preceded the increased expression of  $\alpha$ SMA ( $n = 2$  animals per time point). Quantification of mean of 8–10 confocal images per animal at 200 $\times$  hpf. \* $P < 0.05$ ; \*\*\* $P < 0.001$  by two-way ANOVA test; mean  $\pm$  SD.
- C In the UUO model, COUP-TFII-positive cells do not stain with markers of inflammatory cells (T cell marker CD3, neutrophil marker LyG6, or macrophage marker F4/80;  $n = 3$  animals).
- D–F (D) Protocol for fate tracing of Gli1<sup>+</sup> cells in the UUO model, (E, F) Gli1-tdTomato<sup>+</sup> cells expanded primarily in the outer medullary region. In contrast, COUP-TFII<sup>+</sup> cells are distributed both in cortex and medulla. A subset of COUP-TFII<sup>+</sup> cells (green) overlap with genetically labeled Gli1<sup>+</sup> pericyte/perivascular cells (red) in UUO injury model in the outer medullary region ( $n = 3$  animals per group). CTL: contralateral kidney. Quantification of mean of 8–10 confocal images per animal at 200 $\times$  hpf.

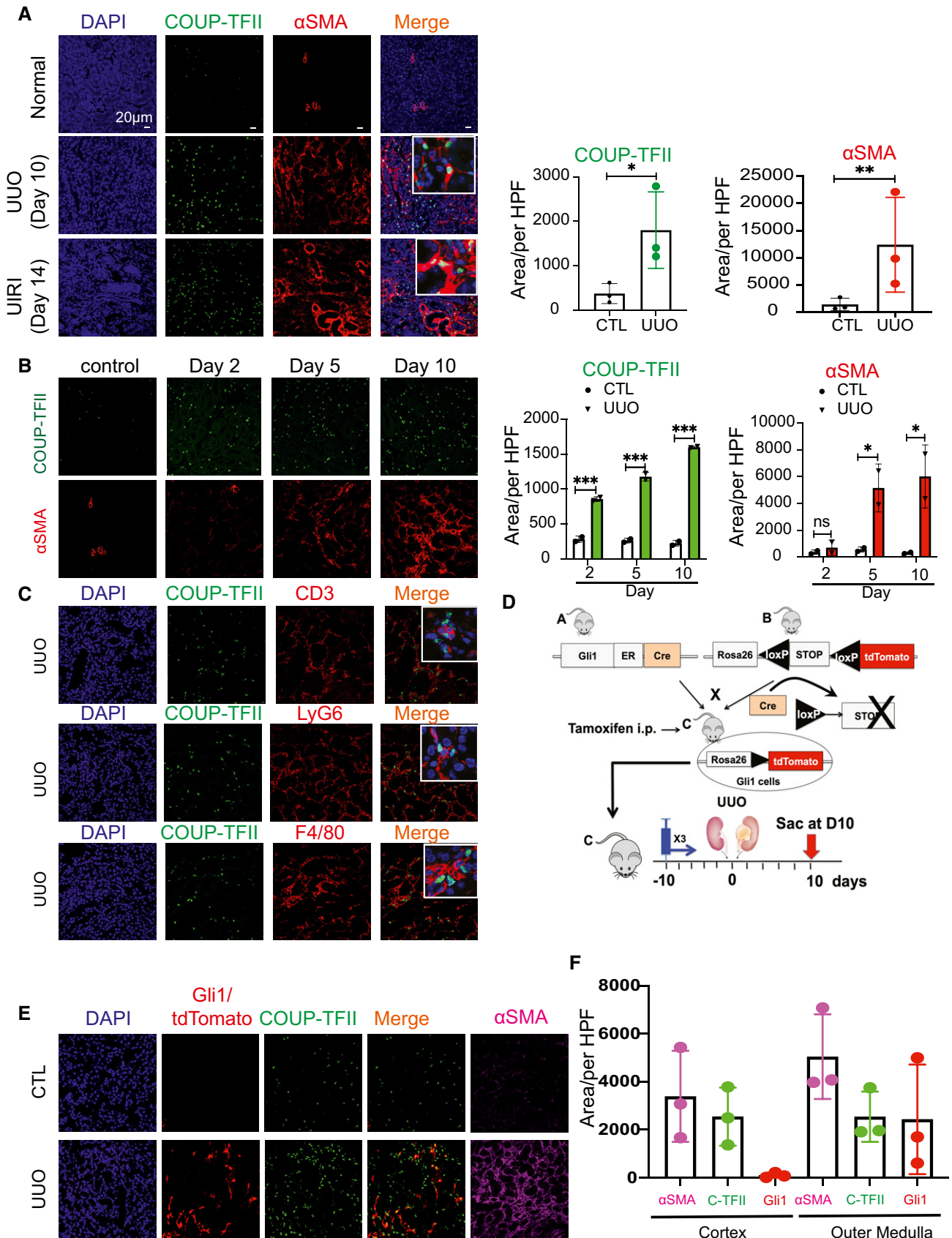


Figure 3.

have glucose and pyruvate. Collectively, these data demonstrated increased glycolysis in COUP-TF OE cells in response to TGF $\beta$ 1 stimulation.

As shown in Fig 6F, TGF $\beta$ 1 up-regulated genes involved in glycolysis, such as glucose transporter 1 (*Glut1*), *HK2*, and lactate dehydrogenase A (*LDHA*), as well as genes activated in fibrosis ( $\alpha$ SMA and *ColA1*). To directly test the link between glycolytic metabolism and myofibroblast differentiation, we treated COUP-TFII OE cells with 2-DG. 2-DG attenuated the TGF $\beta$ 1-induced expression of genes involved in glycolysis, as well as  $\alpha$ SMA and *collagen 1*. We confirmed that 2-DG suppressed TGF $\beta$ 1-induced proteins of  $\alpha$ SMA and *ColA1* in COUP-TFII OE cells without changes in the level of COUP-TFII protein (Fig 6G). These data suggest that COUP-TFII enhances TGF $\beta$ 1-induced glycolysis during myofibroblast differentiation and that the enhancement of glycolysis is essential for this process.

Our proteomic data suggested that COUP-TFII overexpression significantly down-regulated proteins involved in fatty acid oxidation (FAO) pathways (Fig 6A). Among those proteins, pyruvate dehydrogenase kinase 4 (*PDK4*) was significantly decreased in COUP-TFII OE cells in response to TGF $\beta$ 1 (Fig 7A). *PDK4* plays a central role in cellular energy metabolism through inhibition of pyruvate dehydrogenase complex (PDC), a mitochondrial multi-enzyme complex that converts pyruvate to acetylcoenzyme A (AcetylCoA). Glucose and fatty acid compete with each other for oxidation through PDC. Lower *PDK4* leads to greater PDC activity and, therefore, increases in glucose oxidation and inhibition of fatty acid oxidation (Zhang *et al*, 2014). Quantitative real-time PCR data revealed that overexpressing COUP-TFII resulted in decreased transcription of *PGC1 $\alpha$*  and *PDK4*, and knockout of COUP-TFII increased *PGC1 $\alpha$*  and *PDK4* *in vitro* (Fig 7B).

We then asked whether COUP-TFII regulates gene expression of *PGC1 $\alpha$* , *PDK4*, or  $\alpha$ SMA through direct binding to their promoters. Our Chip-qPCR results showed that *PGC1 $\alpha$*  is a target of COUP-TFII, but  $\alpha$ SMA or *PDK4* are not (Fig 7C). Therefore, decreased *PDK4* expression observed with COUP-TFII overexpression might be indirectly due to suppression of *PGC1 $\alpha$*  expression. To determine whether activation of FAO pathways is sufficient to mitigate the effect of COUP-TFII on glycolysis and myofibroblast differentiation, we overexpressed *PGC1 $\alpha$*  through adenovirus transduction in C3H/10T1/2 cells (WT; Fig 7D). As shown in Fig 7E, *PGC1 $\alpha$*  OE significantly increased expression of *Cpt1* and *PDK4*, two key contributors to FAO. However, overexpression of *PGC1 $\alpha$*  did not abrogate the TGF $\beta$ 1 up-regulated genes in glycolysis and  $\alpha$ SMA. Furthermore, we infected COUP-TFII OE cells with the *PGC1 $\alpha$*  adenovirus (Fig 7F). *PGC1 $\alpha$*  OE did not decrease  $\alpha$ SMA protein neither in the absence or presence of TGF $\beta$ 1 in COUP-TFII OE cells. These data suggest that COUP-TFII OE suppressed FAO pathway, although activation of the

FAO pathway is not sufficient to reverse TGF $\beta$ 1-induced glycolysis during myofibroblast differentiation.

Taken together, these data demonstrated that COUP-TFII regulates cell metabolism through suppression of FAO and enhancement of glycolysis in myofibroblasts, thereby promoting myofibroblast differentiation, and collagen 1 production after injury (Fig 7G).

## Discussion

Pericyte/perivascular cells are important contributors to kidney fibrosis after injury (Lin *et al*, 2008; Humphreys *et al*, 2010). These cells are the main source of myofibroblasts, effector cells for fibrosis (Duffield, 2014; Humphreys, 2018). Blocking the differentiation of pericyte/perivascular cells to myofibroblasts is an attractive strategy to reduce fibrosis. TGF $\beta$ , a master regulator of myofibroblast differentiation, has been extensively studied as a therapeutic target (Akhurst & Hata, 2012; Meng *et al*, 2012; Rangarajan *et al*, 2016). Direct inhibition of TGF $\beta$ , however, has led to more toxicity than benefit (Li *et al*, 2006; Principe *et al*, 2014). Therefore, alternative molecular approaches to the regulation of myofibroblast differentiation during fibrosis development are desirable for anti-fibrotic drug development.

We demonstrate that COUP-TFII is markedly increased in human kidneys with fibrosis or cells in human kidney organoids activated with IL-1 $\beta$ , TGF $\beta$ , or cobalt chloride to enhance stromal fibrosis. COUP-TFII is expressed in pericytes/perivascular cells in the adult non-injured kidney and co-localizes with  $\alpha$ SMA expression during fibrosis formation after kidney injury. Our data suggest that COUP-TFII can be a marker of myofibroblasts after injury and be a regulator of myofibroblast differentiation. Another protein proposed to be important in converting pericytes/perivascular cells to myofibroblasts is *Gli1* (Kramann *et al*, 2015). Compared with *Gli1*, COUP-TFII is seen in more  $\alpha$ SMA<sup>+</sup> cells, including many that are not *Gli1*-tdTomato<sup>+</sup>, especially in the kidney cortex. Therefore, COUP-TFII serves a different functional role than *Gli1*. Genetic depletion of COUP-TFII reduced  $\alpha$ SMA-positive cells and attenuated kidney fibrosis after injury. Our results demonstrate that COUP-TFII plays a pivotal role in myofibroblast differentiation and kidney fibrosis. We also show increased COUP-TFII expression in myofibroblasts in fibrotic lungs of patients with idiopathic lung fibrosis (IPF). These findings suggest that the fibrogenic response may share a common pathway in kidney and lung injury and failure.

Our proteomic data revealed that COUP-TFII promotes the expression of proteins enriched in metabolic processes critical for myofibroblasts, in particular, suppression of FAO and enhancement of glycolysis. Our data link COUP-TFII to the metabolism

### Figure 4. Genetic ablation of COUP-TFII in adult mice attenuates injury-induced kidney fibrosis.

- A Strategy of conditional knockdown of COUP-TFII in adult mice. A *LacZ* knock-in allele is inserted into the genomic COUP-TFII locus after the second *LoxP* site.
- B Activation of Cre recombinase by tamoxifen (TAM) results in COUP-TFII deletion and the expression of *LacZ* reporter (detected by immunostaining of  $\beta$ -galactosidase ( $\beta$ -Gal, red) in the UUO mice model ( $n = 2$ ). Quantification of mean of 8–10 confocal images at 200 $\times$  hpf. **\*\* $P < 0.01$** ; **\*\*\* $P < 0.001$**  by paired *t*-test; mean  $\pm$  SD.
- C Using heterozygous mice (*F/+*; Cre/+),  $\beta$ -Gal<sup>+</sup> cells (red) increased after TAM injection in UUO kidneys, and co-localized with COUP-TFII<sup>+</sup> cells (green;  $n = 3$ ).
- D COUP-TFII<sup>+</sup> cells decreased significantly in the UUO kidney in TAM-treated homozygous (*F/F*; Cre/+ ) mice (KO group,  $n = 6$ ) compared with wild-type littermates (WT group,  $n = 4$ ). Expression of  $\alpha$ SMA (red) and collagen 1 (yellow) are also markedly reduced. Masson Trichrome staining shows less kidney fibrosis in KO compared with WT group. Quantification of mean of 8–10 confocal images per animal at 200 $\times$  hpf. **\*\* $P < 0.01$**  by unpaired *t*-test, mean  $\pm$  SD.



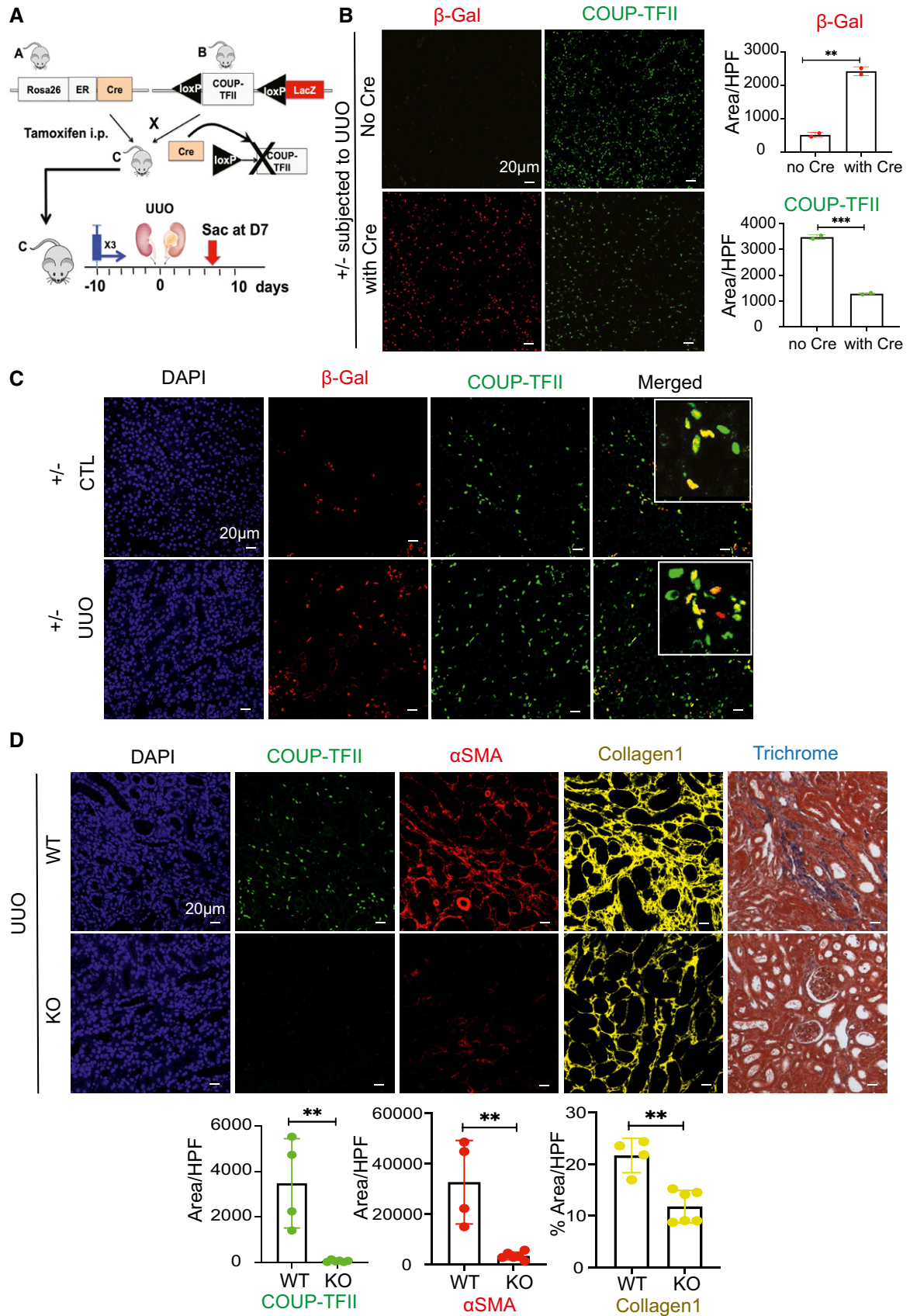


Figure 4.

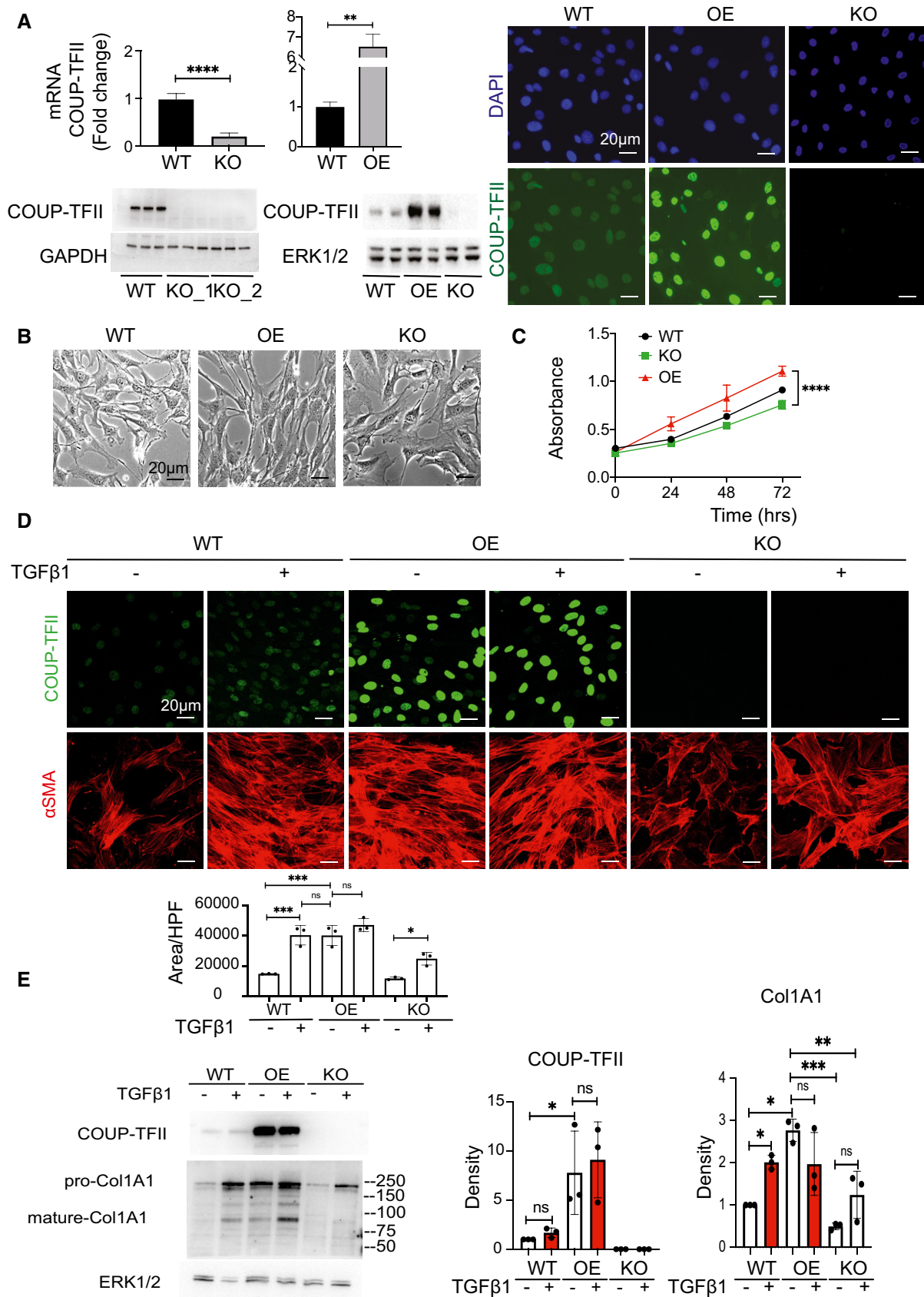


Figure 5.

**Figure 5. Cellular knockout of COUP-TFII *in vitro* in C3H/10T1/2 cells decreases cell proliferation and suppresses TGFβ1-induced αSMA and collagen 1 expression. In contrast, overexpression of COUP-TFII alone increases collagen 1 production.**

- A Verification of COUP-TFII loss- and gain-of-function cell lines generated by CRISPR-Cas9 and an inducible lentiviral construct in pericyte-like cell line C3H/10T1/2 *in vitro* ( $n = 6$ ), \*\*\*\* $P < 0.0001$  by paired *t*-test.
- B, C COUP-TFII KO had no effect on cell viability, although there was decreased proliferation rate compared with naïve C3H/10T1/2 cells (WT;  $n = 6$ ), \*\*\*\* $P < 0.0001$  by two-way ANOVA.
- D COUP-TFII-OE cells, in the absence of TGFβ1 stimulation, displayed an elongated fibroblast shape with increased αSMA expression, similar to WT cells treated with TGFβ1. KO cells had morphology and αSMA expression similar to untreated WT cells. Quantification of mean of 8–10 confocal images at 400× hpf, \* $P < 0.05$ , \*\* $P < 0.01$ , \*\*\* $P < 0.001$  by one-way ANOVA, mean ± SD.
- E Overexpression of COUP-TFII alone without TGFβ1 induces collagen 1 production ( $n = 3$ ). \* $P < 0.05$ , \*\* $P < 0.01$ , \*\*\* $P < 0.001$  by one-way ANOVA, mean ± SD.

deregulation leading to a proliferative and profibrotic function of myofibroblast. Overexpression of COUP-TFII alone (without TGFβ1 treatment) is sufficient to increase glycolysis and collagen 1 expression. Knockout of COUP-TFII dampened TGFβ1-induced glycolysis and decreased αSMA and collagen 1 expression. The phenotypic resemblance between COUP-TFII overexpressed cells and WT cells treated with TGFβ1 suggests that COUP-TFII is essential to establish the myofibroblast phenotype through augmented glycolysis. High glycolytic flux is important for the self-renewal of progenitor cells (Liu *et al*, 2017). Interestingly, COUP-TFII expression is abundant in the mesenchymal compartment of developing organs during embryonic organogenesis but declines significantly right after birth. This suggests that COUP-TFII might be important to maintain the de-differentiation status of cells through augmented glycolysis during development and that injury may recapitulate these developmental programs.

We demonstrated that COUP-TFII increases glycolysis in myofibroblast differentiation. Enhanced glycolysis drives collagen production and fibrosis formation. Besides supporting energy needs in a hypoxic environment, glycolysis also provides macromolecules required for cell proliferation, migration, and amino acid and nucleotide synthesis for DNA replication and RNA transcription (Xie *et al*, 2015; Zhao *et al*, 2019; Henderson *et al*, 2020). In this way, the reprogramming of cell metabolism ensures sufficient building blocks for biosynthesis and facilitates survival and proliferation of myofibroblasts in a harsh hypoxic and nutrient-deprived microenvironment. Furthermore, glycolysis is clearly linked to ECM production (Ding *et al*, 2017; Zhao *et al*, 2019, 2020). Collagen 1, the

predominant structural protein found in kidney fibrosis, is synthesized through multiple steps, including hydroxylation of amino acids, disulfide bonding, and glycosylation (Basak *et al*, 2016). The major amino acid components of collagen are glycine, proline, and lysine. Glycine is mainly produced from glycolysis (de Paz-Lugo *et al*, 2018). In addition, collagen hydroxylation and glycosylation are dependent on glycolysis (Im *et al*, 1976). Our data, together with studies from others (Xie *et al*, 2015; Ding *et al*, 2017), demonstrate that 2-DG (a hexokinase inhibitor) drastically decreases collagen 1 production in myofibroblasts *in vitro*. There is emerging evidence showing that augmented glycolysis in cancer stromal cells (also called cancer-associated fibroblasts) supports cancer progression by secreting lactate and other glycolytic intermediates (Avagliano *et al*, 2018). In addition, a decrease in microenvironmental pH from lactic acid accumulation has been associated with increased TGFβ activity (Kottmann *et al*, 2012). Therefore, targeting glycolysis in myofibroblasts would be expected to not only inhibit the activation of stromal cells, but also to modify the microenvironment of fibrosis foci.

Defective fatty acid oxidation (FAO) plays an important role in mechanisms of renal fibrosis (Kang *et al*, 2015) and DN (Proctor *et al*, 2006). Recent studies revealed that kidney injury down-regulated expression of PGC1α, a master regulator of mitochondrial biogenesis and oxidative metabolism (Tran *et al*, 2016; Dumesic *et al*, 2019). PGC1α knockout mice exhibited more tubular injury and worse renal function after kidney ischemia-reperfusion injury (Tran *et al*, 2016). Overexpression of PGC1α in renal tubular cells provided renal protection (Tran *et al*, 2016; Han *et al*, 2017). We

**Figure 6. COUP-TFII enhances TGFβ1-induced glycolysis during myofibroblast differentiation, which is essential for collagen production *in vitro*.**

- A, B Non-biased proteomics of TGFβ1-treated naïve (WT) and COUP-TFII overexpressing (COUP-TFII-OE) cells revealed that COUP-TFII promotes the expression of proteins enriched in metabolic process critical for myofibroblasts, in particular, suppression of FAO and enhancement of glycolysis. Top pathways ranked by NES (gene set enrichment with FDR < 0.05) altered in COUP-TFII-OE compared with naïve C3H/10T1/2 cells ( $n = 2$ ).
- C TGFβ1 treatment for 48 h significantly increased more lactate production by COUP-TFII-OE (OE) cells when compared to WT or COUP-TFII-KO (KO) cells treated with TGFβ1. Interestingly, overexpression of COUP-TFII alone (without TGFβ1) significantly increased lactate production compared with WT ( $n = 3$ ). \*\* $P < 0.01$ , \*\*\*\* $P < 0.0001$  by one-way ANOVA, mean ± SD. Lactate was released by cells into 100 μl of media.
- D WT, COUP-TFII overexpression (OE), and COUP-TFII knockout (KO) cells were seeded in Seahorse XF-24 cell culture microplates. The cells were rendered quiescent in 0.5% FBS DMEM overnight and then treated with or without 10 ng/ml TGFβ1 for 24 h. All the cells were incubated in the glycolysis stress test medium without glucose and pyruvate, followed by sequential treatments with glucose (10 mM), oligomycin (5 μg/ml), and 2-DG (50 mM). Real-time extracellular acidification rate (ECAR) was recorded as the baseline (before glucose), the rate of glycolysis (after glucose), glycolytic capacity (after oligomycin), and glycolytic reserve (after 2-DG;  $n = 10$ ).
- E With TGFβ treatment COUP-TFII OE significantly increased, while COUP-TFII KO decreased baseline and glucose-stimulated rate of glycolysis, glycolytic capacity, and glycolytic reserve when compared to WT cells. Without TGFβ1 treatment, there is no difference on the baseline and glucose-stimulated glycolysis among WT, OE, and KO cells; however, COUP-TFII KO significantly decreased glycolytic capacity and reserve compared with WT ( $n = 10$ ), \* $P < 0.05$ ; \*\* $P < 0.01$ ; \*\*\*\* $P < 0.0001$  by one-way ANOVA, mean ± SD.
- F 2-deoxyglucose (2-DG) treatment inhibited TGFβ1-induced expression of genes involved in glycolysis (left) and fibrosis (right) in COUP-TFII-OE cells quantitated by qRT-PCR ( $n = 6$ ). \*\* $P < 0.01$ , \*\*\*\* $P < 0.0001$  by one-way ANOVA, mean ± SD. 2-DG suppressed TGFβ1-induced proteins of αSMA and ColA1 in COUP-TFII OE cells without change the protein of COUP-TFII by western blot ( $n = 3$ ). \*\* $P < 0.01$  by one-way ANOVA.

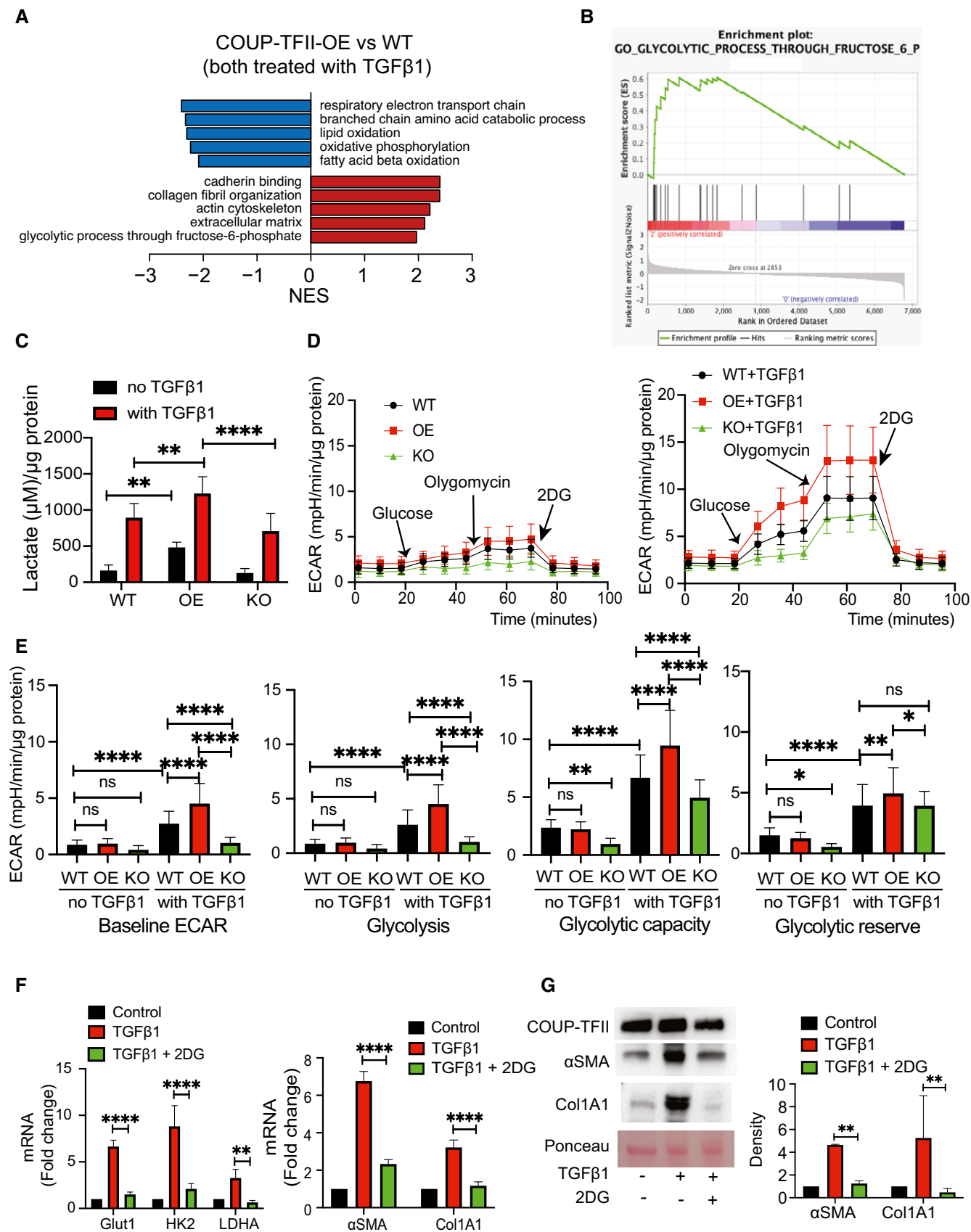


Figure 6.

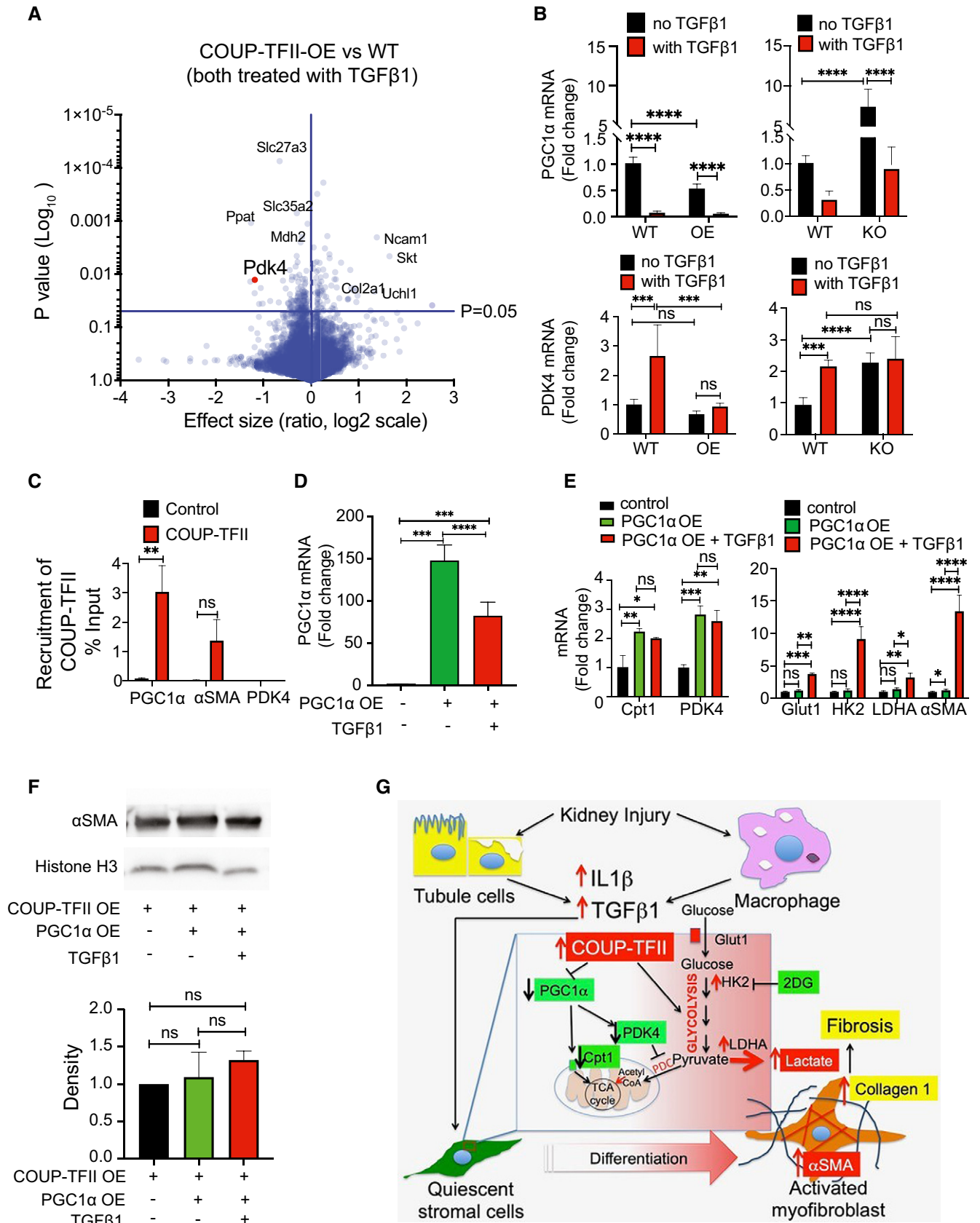


Figure 7.

**Figure 7. Overexpressing COUP-TFII resulted in decreased transcription of PGC1 $\alpha$  and PDK4, and knockout of COUP-TFII increased PGC1 $\alpha$  and PDK4 *in vitro*. Overexpression of PGC1 $\alpha$ , however, is not sufficient to suppress TGF $\beta$ 1-induced glycolysis and COUP-TFII induced myofibroblast differentiation.**

- A Volcano plot of all detected proteins from proteomics of TGF $\beta$ 1-treated naïve (WT) and COUP-TFII overexpressing (COUP-TFII-OE) cells. PDK4 expression is significantly decreased in OE cells ( $n = 2$ ).
- B Without TGF $\beta$  treatment, overexpression of COUP-TFII inhibited, and knockout of COUP-TFII increased, mRNA of PGC1 $\alpha$ . Although overexpression of COUP-TFII did not change the mRNA of PDK4, knockout of COUP-TFII significantly increased the expression of PDK4 ( $n = 6$ ). \*\*\* $P < 0.001$ , \*\*\*\* $P < 0.0001$  by one-way ANOVA, mean  $\pm$  SD.
- C Chip-qPCR analysis on C3H/10T1/2 cells *in vitro* revealed binding of COUP-TFII on the promoter of PGC1 $\alpha$ , but not  $\alpha$ SMA or PDK4 ( $n = 2$ ). \*\* $P < 0.01$ , mean  $\pm$  SD.
- D Overexpression of PGC1 $\alpha$  was achieved through adenovirus transduction in C3H/10T1/2 cells (WT) and confirmed by qRT-PCR ( $n = 6$ ). \*\*\* $P < 0.001$ , \*\*\*\* $P < 0.0001$  by one-way ANOVA, mean  $\pm$  SD.
- E PGC1 $\alpha$  OE significantly increased expression of Cpt1 and PDK4. Both are involved in key steps of FAO. However, overexpression of PGC1 $\alpha$  did not abrogate the TGF $\beta$ 1 up-regulated glycolytic genes and  $\alpha$ SMA ( $n = 6$ ). \* $P < 0.05$ ; \*\* $P < 0.01$ ; \*\*\*\* $P < 0.0001$  by one-way ANOVA, mean  $\pm$  SD.
- F PGC1 $\alpha$  OE did not decrease  $\alpha$ SMA protein neither with nor without TGF $\beta$ 1 in COUP-TFII OE cells by Western Blot analysis ( $n = 3$ ).
- G Schematic model of the role of COUP-TFII in metabolic reprogramming during myofibroblast differentiation and fibrosis formation after injury. PDC: pyruvate dehydrogenase complex.

found that COUP-TFII OE significantly decreased, while COUP-TFII KO increased, transcription of PGC1 $\alpha$  in C3H/10T1/2 cells. Our Chip-qPCR results revealed that COUP-TFII directly binds to the PGC1 $\alpha$  promoter, consistent with other reports (Li *et al*, 2009; Wu *et al*, 2015). Therefore, we speculate that COUP-TFII-mediated suppression of FAO may relate to decreased PGC1 $\alpha$  expression. In our experiments, overexpression of PGC1 $\alpha$  increased the expression of PDK4 and Cpt1, key components of FAO (Zhang *et al*, 2014; Schlaepfer & Joshi, 2020). PGC1 $\alpha$  overexpression, however, did not suppress TGF $\beta$ -induced glycolysis and fibrosis in myofibroblasts. Furthermore, overexpression of PGC1 $\alpha$  did not reverse the effect of COUP-TFII overexpression on  $\alpha$ SMA production. Therefore, enhanced glycolysis by COUP-TFII is not dependent on decreases in expression of PGC1 $\alpha$ . COUP-TFII can drive glycolysis and myofibroblast differentiation even in the absence of reductions in PGC1 $\alpha$  expression. Renal proximal tubular cells are well known to depend mainly on oxidative metabolism. PGC1 $\alpha$  overexpression is protective but this may be due to protection during the injury phase (Tran *et al*, 2016; Han *et al*, 2017). In contrast, podocytes and fibroblasts rely on glycolysis (Rabelink & Carmeliet, 2018; Brinkkoetter *et al*, 2019). Therefore, overexpression PGC1 $\alpha$  in fibroblast might not be sufficient to suppress TGF $\beta$ 1-induced glycolysis and COUP-TFII induced myofibroblast differentiation.

Since COUP-TFII is expressed primarily in myofibroblasts, targeting it may be selectively effective to suppress myofibroblast differentiation and function without affecting epithelial or endothelial cells. There are no overt phenotypes in mice where COUP-TFII has been knocked out at the adult stage (Xie *et al*, 2016; Ceni *et al*, 2017) further supporting the potential safety profile of COUP-TFII inhibition. We demonstrate that COUP-TFII is markedly increased in stroma cells in human kidney organoids treated with IL-1 $\beta$ , TGF $\beta$ , or CoCl<sub>2</sub>, which mimic inflammation or ischemia during injury. These *ex vivo* human cell systems can be used to test potential inhibitors of COUP-TFII.

In conclusion, our study provides compelling evidence that COUP-TFII regulates myofibroblast differentiation and fibrosis in models of kidney injury. The profibrotic function is mediated through augmented glycolysis and resultant differentiation of pericytes/fibroblasts to myofibroblast after injury. Reducing COUP-TFII is effective in diminishing myofibroblast differentiation and limiting fibrosis *in vivo*. The fibrogenic response may share a common pathway in different organ systems. Targeting COUP-TFII may serve as a novel treatment approach for mitigating fibrosis in chronic kidney disease and fibrosis of other organs.

## Materials and Methods

### Human kidney biopsy sample preparation and immunostaining

Normal kidney samples used for immunostaining studies were obtained from surgical sections from patients undergoing nephrectomy due to renal cell carcinoma (RCC) under institutional review board-approved protocols. Injured kidney samples were obtained from kidney biopsy samples from patients with TMA and DN.

### Human kidney organoids generation and IL-1 $\beta$ stimulation

Kidney organoids were derived from H9 human embryonic stem cells as previously described (Morizane *et al*, 2015). Briefly, H9 cells were cultured in StemFit (Ajinomoto) supplemented with 10 ng/ml FGF2 (PeproTech). Differentiation was started with 8  $\mu$ M CHIR (TOCRIS) for 4 days, followed sequentially by Activin for 3 days and FGF9 for 1–2 days. Subsequently, cells were dissociated with Accutase (Stem Cell Technologies) and plated into U-shaped bottoms 96-well plates (Corning) at 100,000 cells per well in a medium supplemented with 3  $\mu$ M CHIR and 10 ng/ml FGF9. Two days later, the medium was changed to one supplemented with only 10 ng/ml FGF9. After 3–4 days, the medium was changed to basal medium without additional growth factors. At day 51, matured organoids were treated with IL-1 $\beta$  10 ng/ml (Sigma) for 96 h. Organoids were collected and fixed in 4% PFA for 30 min followed by 20% sucrose overnight. Cryosections (7  $\mu$ m) were incubated with antibodies for immunofluorescence. Images were captured by confocal microscopy using a Nikon C1 microscope running EZ-C1 software.

### Mouse strain and animal experiments

All mouse experiments were performed under the animal use protocol approved by the Institutional Animal Care and Use Committee of the Brigham and Women's hospital. *Gli1-CreER<sup>2</sup>* (JAX# 007913), *Rosa26tdTomato* (JAX# 007909), *Foxd1-GFP-Cre* (Jax# 012463), and *Rosa26-CreER<sup>2</sup>* (JAX# 008463) were purchased from Jackson Laboratories (Bar harbor, ME). COUP-TFII flox/+ mice were purchased from Mutant Mouse Resource & Research Centers (MMRRC; B6;129S7-Nr2f2tm2Tsa/Mmmh, Cat# 032805-MU). The COUP-TFII flox/+ mouse strain was maintained in a mixed genetic background (129/Sv  $\times$  C57BL/6) and received standard rodent chow. To induce COUP-TFII deletion in the adult, 8- to 12-week-old mice were intraperitoneally injected with three doses 0.1 mg/g body weight

tamoxifen in corn oil/3% ethanol (Sigma) every other day starting 14 days before surgery.

Murine kidney fibrosis models were performed as previously described (Yang *et al*, 2010). Briefly, mice were anesthetized with pentobarbital sodium (60 mg/kg body weight, intraperitoneally). For the unilateral ureteral obstruction (UUO) surgery, a flank incision was made and the left ureter was tied off at the level of the lower pole with two 4.0 silk ties. For the unilateral ischemia-reperfusion injury (IRI), the left kidney was exposed through a flank incision and subjected to ischemia by clamping the renal pedicle with non-traumatic micro-aneurysm clamps (Roboz, Rockville, MD) for 30 min. Reperfusion was confirmed by visual color change. Body temperatures were controlled at 36.5–37.5°C throughout the procedure. One milliliter of warm (body temperature) saline was instilled in the retroperitoneum after surgery for volume supplementation. Buprenorphine was used for pain control (0.1 mg/kg body weight, intraperitoneally). Mice were sacrificed at day 2, 5, or 10 after UUO and day 14 after unilateral IRI.

### Histology and immunofluorescence staining

Mice were anesthetized with isoflurane (Baxter) and subsequently perfused via the left ventricle with 4°C PBS for 1 min. Kidneys from adult mice were fixed with 4% paraformaldehyde (PFA), dehydrated, and embedded in paraffin. Hematoxylin/eosin, PAS, and Masson's trichrome staining were performed using standard protocols (Yang *et al*, 2010).

Immunofluorescence staining of mouse kidneys was performed on paraffin sections as previously described (Yang *et al*, 2010). Briefly, the tissue sections were deparaffinized, followed by antigen retrieval and rehydration. Then tissue antigens were labeled with primary antibodies to COUP-TFII (Abcam, diluted 1:200),  $\alpha$ SMA (Sigma, 1:400), collagen 1 (EMD Millipore, 1:400), CD31 (Abcam 1:200), PDGF receptor beta (PDGFR $\beta$ , Abcam 1:400), or  $\beta$ -galactosidase (Abcam 1:100), followed by FITC or Cy3-labeled secondary antibodies (Jackson ImmunoResearch). Some immunostaining was performed on frozen sections. Cryosections (7  $\mu$ m) were fixed in 4% PFA for 2 h and then washed in 30% sucrose solution overnight. Primary antibodies used in cryosections recognized the following proteins: CD3 (eBioscience 1:100), LyG6, and F4/80 (Thermo Fisher). Images were captured by a confocal (Nikon C1) or standard fluorescent microscope (Nikon TE 1000).

### Cell culture and treatment

The C3H/10T1/2 (American Type Culture Collection) were cultured in DMEM medium supplemented with 10% FBS until the cells were 80% confluent. Cell morphology was examined and captured using live cell imaging (Nikon). For induction of myofibroblast differentiation, subconfluent cells were incubated in DMEM medium containing 0.5% FBS overnight, then treated with TGF $\beta$ 1 (10ng/ml; R&D).

### CRISPR/Cas9 knockout

COUP-TFII guide RNAs were created using a guide design web tool (<http://crispr.mit.edu>): COUP-TFII guide 1, TATATCCGGACAGG TACGAG; COUP-TFII guide 2, GAGGGGGTCCCCGTTGGTCA. sgRNA oligos were cloned into pSpCas9(BB)-2A-GFP (Addgene, 48138). The protocol was performed according to published

methods (Ran *et al*, 2013). C3H/10T1/2 cells ( $5 \times 10^4$ ) were transfected with lipofectamine 3000. Cells were grown for 48 h and then sorted for GFP and positive cells seeded as single cells in 96-well plates. Cells were then returned to the incubator, and cultures were allowed to expand for 2–3 weeks.

### Tet-inducible COUP-TFII expression

To generate a lentiviral transfer plasmid for inducible gain-of-function experiments, we used high-fidelity PCR (iProof, Bio-Rad) to amplify full-length mouse COUP-TFII cDNA, flanked with attB1 and attB2 sites on 5' and 3' ends, respectively, from a cDNA library from adult mouse kidney. The resulting PCR band was purified from a 0.8% agarose gel using the QIAquick Gel Extraction kit (Qiagen). The purified PCR product was then cloned into pDONR221 (Thermo Fisher Scientific) using BP Clonase II (Invitrogen) according to manufacturer's instructions. We then shuttled the COUP-TFII cDNA into the destination vector pInducer20 (a gift from Stephen Elledge, Addgene #44010) using LR Clonase II (Invitrogen). All cloning steps were verified using Sanger sequencing (Genewiz, Inc.). C3H/10T1/2 cells were infected with lentivirus in the presence of 10  $\mu$ g/ml polybrene (Sigma). Infected cells were selected with puromycin (Sigma).

### Adenovirus-mediated PGC1 $\alpha$ expression

Adenovirus encoding GFP or tagless mouse PGC1 $\alpha$  (PGC1 $\alpha$ 1 isoform, (Ruas *et al*, 2012)) was made using the virapower adenoviral expression system (invitrogen) and titered using the adeno-x rapidtiter kit (clontech). C3H/10T1/2 cells were transduced with an adenovirus at an MOI of 300 overnight.

### Cell proliferation assay

Cells were seeded on a 96-well plate at a concentration of  $1 \times 10^4$  per well. Three parallel wells of cells were studied for each group. After incubation for 1, 2, or 3 days, 20  $\mu$ l MTT ((3-(4,5-Dimethyl-2-thiazolyl)-2,5-diphenyltetrazolium Bromide), promega) was added. After 2 h of MTT exposure, cells were washed and subjected for colorimetric measurement. The OD values were obtained by a microplate reader (SpectraMax M5, Molecular Devices) at 570 nm.

### Quantitative real-time PCR (qRT-PCR)

At indicated times, total RNA was extracted using TRIzol (Sigma) as described (Yang *et al*, 2010). Subsequently, 2  $\mu$ g of total RNAs was reverse-transcribed to cDNA with random primers using reverse transcriptase (Invitrogen). A 1:5 dilution of cDNA was then amplified by real-time qPCR in a CFX96 real-time system (Bio-Rad) using SYBR green. Relative gene expression was calculated by the  $\Delta\Delta$ Ct method, and final results were expressed as the fold difference relative to control conditions in gene expression normalized to Ribosomal Protein L32 (RPL32). Primers for individual gene expression were listed in Table 1.

### ChIP assay

Chromatin immunoprecipitation and real-time PCR quantification were performed as described (Mukhopadhyay *et al*, 2008). The

**Table 1. Primers for qRT-PCR and ChIP-qPCR.**

Target	Primer	Sequence
qRT-PCR		
mRPL32	Forward	GCTGCCATCTGTTTTACGG
mRPL32	Reverse	TGACTGGTGCCTGATGAAC
mHexokinase 2	Forward	CAACTCCGGATGGGACAG
mHexokinase 2	Reverse	CACACGGAAGTTGGTTCCTC
mGlut1	Forward	GCT TCT CCA ACT GGA CCT CAA AC
mGlut1	Reverse	ACG AGG AGC ACC GTG AAG ATG A
mLDHA	Forward	ACGCAGACAAGGAGCAGTGGAA
mLDHA	Reverse	ATGCTCTCAGCCAAGTCTGCCA
mPGC1 $\alpha$	Forward	AGTCCATACACAACCGCAG
mPGC1 $\alpha$ _	Reverse	CCCTTGGGGTCATTTGGTGA
m $\alpha$ SMA	Forward	CTGACAGAGGCACCACTGAA
m $\alpha$ SMA	Reverse	CATCTCCAGAGTCCAGCACA
mCollagen1	Forward	TGACTGGAAGAGCGGAGAGT
mCollagen1	Reverse	GTTCGGGCTGATGTACCAGT
ChIP-qPCR		
mPGC1 $\alpha$	Forward	TTGCCTCCCTCTACCTAC
mPGC1 $\alpha$	Reverse	GCATGTTTGTCTGGTTCGCTA
mPDK4	Forward	GATCCCGACACGGTTTCCAT
mPDK4	Reverse	AAGTCTAGCGACCTGGGAT
m $\alpha$ SMA	Forward	TGTAGCCGTAGCATCTTGCC
m $\alpha$ SMA	Reverse	TAACCAACACACCAGGAGCC

rabbit polyclonal COUP-TFII antibody (Millipore, Cat# ABE 1426) and rabbit IgG1 antibody (Zymed) were used for immunoprecipitation. After purification of DNA from C3H/10T1/2 cells, bound sequences were determined by quantitative real-time PCR (Table 1 for the primer sequences for the ChIP assay).

### Western Blot analysis

48 h after transfection, C3H/10T1/2 cells were lysed with 1xRIPA buffer containing a protease inhibitor cocktail (Roche Applied Science) for 30 min on ice. After centrifugation for 15 min, the supernatant was collected, and protein content of the samples was analyzed according to the Bradford method. Proteins were loaded onto SDS-polyacrylamide gels and blotted onto PVDF membrane (Bio-Rad Laboratories). Western blots were performed using antibodies directed against COUP-TFII (abcam, 1: 2,000),  $\alpha$ SMA (Sigma, 1:4,000), and ERK2 (Cell signaling). HRP-conjugated secondary antibodies were purchased from DAKO. Enhanced chemiluminescence was performed according to the manufacturer's instructions. ERK1/2 protein was used to ensure equivalent loading of protein samples.

### Proteomics

Naïve (WT) and COUP-TFII overexpression (OE) cells were both treated with TGF $\beta$ 1 (10 ng/ml) for 48 h to induce myofibroblast differentiation. After trypsinization, cells were washed twice in PBS. Cell pellets were frozen in  $-80^{\circ}\text{C}$  for proteomics experiments.

### Protein extraction and digest

PBS was removed, followed by the addition of SDS lysis buffer (2% SDS, 150 mM NaCl, 50 mM Tris, pH 8.7) containing protease inhibitors (Complete, Roche). Lysates were homogenized over Qiashredder columns (Qiagen, ref. 79656) and centrifuged at 16,000 g for 1 min at room temperature. Reductive methylation of cysteine residues was performed by adding dithiothreitol (DTT) to a final concentration of 5 mM and heating to  $37^{\circ}\text{C}$  for 1 h, followed by alkylation with iodoacetamide at a final concentration of 15 mM and incubation at room temperature in the dark for 30 min and quenching with DTT. Protein concentration was determined using a Micro BCATM Protein Assay Kit (Thermo Fisher, Catalog# 23235). Detergent was removed by methanol/chloroform protein precipitation as described previously (Wessel & Flugge, 1984). Lys-C protease digests (Wako, Catalog# 129-02541) in 2 M urea 20 mM EPPS, pH 8.5 at  $37^{\circ}\text{C}$  for 3 h were followed by further digestion at  $37^{\circ}\text{C}$  for 6 h with trypsin (Promega, Catalog# V5113). Missed cleavage rate was determined by LC-MS/MS.

### Tandem mass tag labeling, ratio check and HPLC fractionation

Equal amounts of protein were removed from each sample and labeled using a TMT11plex Mass Tag Labeling Kit (Thermo Fisher, Catalog# A34808). Tandem mass tag (TMT) labeling efficiency and ratio checks were determined by LC-MS3 analysis. Quenched TMT labeling reactions were combined and de-salted using a SepPak tC18 Vac RC Cartridge (50 mg, Waters, Catalog# WAT054960). HPLC fractionation was performed using an Agilent 1200 Series instrument with a flow rate of 600  $\mu\text{l}/\text{min}$  over a period of 75 min. Peptides were collected in a 96-well plate over a 65 min-gradient of 13–44 %B with Buffer A comprising 5% acetonitrile, 10 mM ammonium bicarbonate, pH 8 and Buffer B comprising 90% acetonitrile, 10 mM ammonium bicarbonate, pH 8. Fractions were then pooled into 24 samples, followed by sample cleanup using the Stage Tip protocol. This protocol uses C18 Empore<sup>TM</sup> Extraction Disks (Fisher Scientific, Catalog# 14-386-2). Samples were dried before re-suspension in MS Loading Buffer (3% acetonitrile, 5% FA).

### LC-MS

Peptides were separated over a 30 cm, 100  $\mu\text{m}$  (internal diameter) column using an EASY-nLC 1200 HPLC system. Samples from the HPLC were injected into an Orbitrap Fusion Lumos Tribrid MS (Thermo Fisher, Catalog# FSN02-10000) and measured using a multi-notch MS3 method (Ting *et al*, 2011; McAlister *et al*, 2014). MS scans were performed in the Orbitrap over a scan range of 400–1,400  $m/z$ . The top 10 ions with charge states from 2 to 6 were selected for MS/MS. Turbo rate scans were performed in the Ion Trap with a collision energy of 35% and a maximum injection time of 250 ms. TMT quantification was performed using SPS-MS3 in the Orbitrap with a scan range of 100–1,000  $m/z$ , and an HCD collision energy of 55%. Orbitrap resolution was 50,000 (dimensionless units) with a maximum injection time of 300 ms.

### Proteomic data analysis

Raw data were converted to mzXML format and peptide ID used Sequest (Eng *et al*, 1994) (version 28 ([http://fields.scripps.edu/yates/wp/?page\\_id=17](http://fields.scripps.edu/yates/wp/?page_id=17))) with searches against the mouse proteome UniProt database (July 2014). The database search included reversed protein sequences and known contaminants such as keratins that were excluded for subsequent analyses. Linear discriminant



analysis was performed (Elias & Gygi, 2007) and peptide false discovery rate (FDR) was < 1% after applying a target-decoy database search strategy. Filtering was performed as described previously (McAlister et al, 2014). Variable modification for oxidized methionine (+15.99 Da) was used during searches. For protein identification and quantification, shared peptides were collapsed into the minimally sufficient number of proteins using rules of parsimony. Peptides with a total TMT value of > 200 and an isolation specificity of > 0.7 were included for quantification.

### Gene set enrichment analysis

We analyzed our proteome datasets from four independent experiments (WT and COUP-TFII-OE, all in duplicates) using the GSEA software developed by Broad Institute (Cambridge, MA) (Subramanian et al, 2005). All the analyses were performed in default setting based on all GO terms (c5.all.v7.0.symbols.gmt).

### Real-time cell metabolism assay

Naïve (WT), COUP-TFII-OE and COUP-TFII-KO C3H/10T1/2 cells were plated in XF-24 Cell Culture Microplates (Seahorse Bioscience) at a cellular density of 20,000 cells per well, then serum starved for 24 h, and stimulated with or without TGFβ1 (10 ng/ml) for 24 h. Real-time analysis of extracellular acidification rate (ECAR) was analyzed using XF Extracellular Flux Analyzer (Seahorse Bioscience). The cells were incubated in basal media followed by sequential injections with glucose (10 mM), oligomycin (5 μg/ml), and 2-DG (50 mM).

### Extracellular lactate assays

Naïve (WT), COUP-TFII-OE, and COUP-TFII-KO C3H/10T1/2 cells were grown in a 96-well plate until 80% confluent, then serum-starved for 24 h, and stimulated with or without TGFβ1 (10 ng/ml) for 48 h in 100 μl DMEM media. Extracellular levels of lactate were determined using the lactate assay kit (BioVision, Milpitas, CA) according to the manufacturer's instructions.

### Statistical analysis

Results are expressed as mean ± SD. Group means were compared by one-way analysis of variance (ANOVA), followed by the Tukey post-test using GraphPad Prism (GraphPad software) for multiple comparisons or by Student's *t*-test. A *P* value < 0.05 was considered statistically significant.

## Data availability

The proteomics data from this publication have been deposited to the PRIDE archive and can be accessed under ProteomeXchange accession number: PXD024035 (<http://www.ebi.ac.uk/pride/archive/projects/PXD024035>).

**Expanded View** for this article is available online.

### Acknowledgements

This work was supported by the National Institutes of Health, National Institutes of Diabetes, Digestive and Kidney Diseases (NIDDK) Grants R37DK039773,

R01DK072381 and UH3TR002155 (to J.V.B.), National Institute of Biomedical Imaging and Bioengineering (NIBIB), Organ Design and Engineering Training Grant 1T32EB016652, Dialysis Clinics (2019-06) (to L.L.). P.G. received support from Monahan Foundation, Fondation pour la Recherche Médicale, Groupe Pasteur Mutualité, Société Francophone de Transplantation, Arthur Sachs fellowship, Philippe Foundation, Fulbright Scholarship, ATIP Avenir program. X.X. was supported by China Scholarship Council fellowship. We thank Dr. Edy Kim from Brigham and Women's hospital who provided human idiopathic pulmonary fibrosis samples for immunostaining. We thank Xiaoming Sun for providing technique support on mice kidney injury models. N.N.L. received support from a NIH training grant (T32HL007609).

### Author contributions

Experiment design: LL and JVB; Experiments: LL, PG, XX, ACF-R, DT, MK, DG-S, MSC, NNL, TI, YM, MTV, JW, and DRL; Proteomic data analysis: MK and JJ-KL; Manuscript writing: LL; Manuscript revision: LL, PG, JVB, ERE, and KWM; Preparation and reading the manuscript: All authors.

### Conflict of interest

Dr. Bonventre is cofounder and holds equity in Goldfinch Bio. He is co-inventor on KIM-1 and kidney organoid patents assigned to Mass General Brigham. Dr. Bonventre's interests were reviewed and are managed by BWH and Partners HealthCare in accordance with their conflict of interest policies. The other authors declare that they have no conflict of interest.

## References

- Akhurst RJ, Hata A (2012) Targeting the TGFβ signalling pathway in disease. *Nat Rev Drug Discov* 11: 790–811
- Ashraf UM, Sanchez ER, Kumarasamy S (2019) COUP-TFII revisited: Its role in metabolic gene regulation. *Steroids* 141: 63–69
- Avagliano A, Granato G, Ruocco MR, Romano V, Belviso I, Carfora A, Montagnani S, Arcucci A (2018) Metabolic reprogramming of cancer associated fibroblasts: the slavery of stromal fibroblasts. *Biomed Res Int* 2018: 6075403
- Bao Y, Gu D, Feng W, Sun X, Wang X, Zhang X, Shi Q, Cui G, Yu H, Tang C et al (2014) COUP-TFII regulates metastasis of colorectal adenocarcinoma cells by modulating Snail1. *Br J Cancer* 111: 933–943
- Basak T, Vega-Montoto L, Zimmerman LJ, Tabb DL, Hudson BG, Vanacore RM (2016) Comprehensive characterization of glycosylation and hydroxylation of basement membrane collagen IV by high-resolution mass spectrometry. *J Proteome Res* 15: 245–258
- Bonventre JV, Yang L (2011) Cellular pathophysiology of ischemic acute kidney injury. *J Clin Invest* 121: 4210–4221
- Brinkkoetter PT, Bork T, Salou S, Liang W, Mizi A, Özel C, Koehler S, Hagmann HH, Ising C, Kuczkowski A et al (2019) Anaerobic glycolysis maintains the glomerular filtration barrier independent of mitochondrial metabolism and dynamics. *Cell Rep* 27: 1551–1566.e1555
- Ceni E, Mello T, Polvani S, Vasseur-Cognet M, Tarocchi M, Tempesti S, Cavalieri D, Beltrame L, Marroncini G, Pinzani M et al (2017) The orphan nuclear receptor COUP-TFII coordinates hypoxia-independent proangiogenic responses in hepatic stellate cells. *J Hepatol* 66: 754–764
- Chen X, Qin J, Cheng CM, Tsai MJ, Tsai SY (2012) COUP-TFII is a major regulator of cell cycle and Notch signaling pathways. *Mol Endocrinol* 26: 1268–1277
- Ding H, Jiang L, Xu J, Bai F, Zhou Y, Yuan Q, Luo J, Zen K, Yang J (2017) Inhibiting aerobic glycolysis suppresses renal interstitial fibroblast activation and renal fibrosis. *Am J Physiol Renal Physiol* 313: F561–F575

- Duffield JS, Lupher M, Thannickal VJ, Wynn TA (2013) Host responses in tissue repair and fibrosis. *Annu Rev Pathol* 8: 241–276
- Duffield JS (2014) Cellular and molecular mechanisms in kidney fibrosis. *J Clin Invest* 124: 2299–2306
- Dumesic PA, Egan DF, Gut P, Tran MT, Parisi A, Chatterjee N, Jedrychowski M, Paschini M, Kazak L, Wilensky SE *et al* (2019) An evolutionarily conserved uORF regulates *pgc1 $\alpha$*  and oxidative metabolism in mice, flies, and Bluefin tuna. *Cell Metab* 30: 190–200.e196
- Elias JE, Gygi SP (2007) Target-decoy search strategy for increased confidence in large-scale protein identifications by mass spectrometry. *Nat Methods* 4: 207–214
- Eng JK, McCormack AL, Yates JR (1994) An approach to correlate tandem mass spectral data of peptides with amino acid sequences in a protein database. *J Am Soc Mass Spectrom* 5: 976–989
- Falke LL, Gholizadeh S, Goldschmeding R, Kok RJ, Nguyen TQ (2015) Diverse origins of the myofibroblast-implications for kidney fibrosis. *Nat Rev Nephrol* 11: 233–244
- Fang X, Liu CX, Zeng XR, Huang XM, Chen WL, Wang Y, Ai F (2020) Orphan nuclear receptor COUP-TFII is an oncogenic gene in renal cell carcinoma. *Clin Transl Oncol* 22: 772–781
- Han SH, Wu MY, Nam BY, Park JT, Yoo TH, Kang SW, Park J, Chinga F, Li SY, Susztak K (2017) PGC-1 $\alpha$  protects from notch-induced kidney fibrosis development. *J Am Soc Nephrol* 28: 3312–3322
- Henderson J, Duffy L, Stratton R, Ford D, O'Reilly S (2020) Metabolic reprogramming of glycolysis and glutamine metabolism are key events in myofibroblast transition in systemic sclerosis pathogenesis. *J Cell Mol Med* 24: 14026–14038
- Hou W, Syn WK (2018) Role of metabolism in hepatic stellate cell activation and fibrogenesis. *Front Cell Dev Biol* 6: 150
- Humphreys BD, Valerius MT, Kobayashi A, Mugford JW, Soeung S, Duffield JS, McMahon AP, Bonventre JV (2008) Intrinsic epithelial cells repair the kidney after injury. *Cell Stem Cell* 2: 284–291
- Humphreys BD, Lin SL, Kobayashi A, Hudson TE, Nowlin BT, Bonventre JV, Valerius MT, McMahon AP, Duffield JS (2010) Fate tracing reveals the pericyte and not epithelial origin of myofibroblasts in kidney fibrosis. *Am J Pathol* 176: 85–97
- Humphreys BD (2018) Mechanisms of renal fibrosis. *Annu Rev Physiol* 80: 309–326
- Im MJ, Freshwater MF, Hoopes JE (1976) Enzyme activities in granulation tissue: energy for collagen synthesis. *J Surg Res* 20: 121–125
- Jha V, Garcia-Garcia G, Iseki K, Li Z, Naicker S, Plattner B, Saran R, Wang AY, Yang CW (2013) Chronic kidney disease: global dimension and perspectives. *Lancet* 382: 260–272
- Kale S, Hanai J, Chan B, Karihaloo A, Grotendorst G, Cantley L, Sukhatme VP (2005) Microarray analysis of *in vitro* pericyte differentiation reveals an angiogenic program of gene expression. *FASEB J* 19: 270–271
- Kang HM, Ahn SH, Choi P, Ko Y-A, Han SH, Chinga F, Park ASD, Tao J, Sharma K, Pullman J *et al* (2015) Defective fatty acid oxidation in renal tubular epithelial cells has a key role in kidney fibrosis development. *Nat Med* 21: 37–46
- Klingberg F, Hinz B, White ES (2013) The myofibroblast matrix: implications for tissue repair and fibrosis. *J Pathol* 229: 298–309
- Kobayashi A, Mugford JW, Krautzberger AM, Naiman N, Liao J, McMahon AP (2014) Identification of a multipotent self-renewing stromal progenitor population during mammalian kidney organogenesis. *Stem Cell Rep* 3: 650–662
- Kottmann RM, Kulkarni AA, Smolnycki KA, Lyda E, Dahanayake T, Salibi R, Honnons S, Jones C, Isern NG, Hu JZ *et al* (2012) Lactic acid is elevated in idiopathic pulmonary fibrosis and induces myofibroblast differentiation via pH-dependent activation of transforming growth factor-beta. *Am J Respir Crit Care Med* 186: 740–751
- Kramann R, Schneider RK, DiRocco DP, Machado F, Fleig S, Bondzie PA, Henderson JM, Ebert BL, Humphreys BD (2015) Perivascular Gli1+ progenitors are key contributors to injury-induced organ fibrosis. *Cell Stem Cell* 16: 51–66
- Lan R, Geng H, Singha PK, Saikumar P, Bottinger EP, Weinberg JM, Venkatachalam MA (2016) Mitochondrial pathology and glycolytic shift during proximal tubule atrophy after ischemic AKI. *J Am Soc Nephrol* 27: 3356–3367
- Lemos DR, McMurdo M, Karaca G, Wilflingseder J, Leaf IA, Gupta N, Miyoshi T, Susa K, Johnson BG, Soliman K *et al* (2018) Interleukin-1 $\beta$  activates a MYC-dependent metabolic switch in kidney stromal cells necessary for progressive tubulointerstitial fibrosis. *J Am Soc Nephrol* 29: 1690–1705
- Li MO, Wan YY, Sanjabi S, Robertson AK, Flavell RA (2006) Transforming growth factor-beta regulation of immune responses. *Annu Rev Immunol* 24: 99–146
- Li L, Xie X, Qin J, Jeha GS, Saha PK, Yan J, Haueter CM, Chan L, Tsai SY, Tsai MJ (2009) The nuclear orphan receptor COUP-TFII plays an essential role in adipogenesis, glucose homeostasis, and energy metabolism. *Cell Metab* 9: 77–87
- Lin SL, Kisseleva T, Brenner DA, Duffield JS (2008) Pericytes and perivascular fibroblasts are the primary source of collagen-producing cells in obstructive fibrosis of the kidney. *Am J Pathol* 173: 1617–1627
- Liu J, Edgington-Giordano F, Dugas C, Abrams A, Katakam P, Satou R, Saifudeen Z (2017) Regulation of nephron progenitor cell self-renewal by intermediary metabolism. *J Am Soc Nephrol* 28: 3323–3335
- Madisen L, Zwingman TA, Sunkin SM, Oh SW, Zariwala HA, Gu H, Ng LL, Palmiter RD, Hawrylycz MJ, Jones AR *et al* (2010) A robust and high-throughput Cre reporting and characterization system for the whole mouse brain. *Nat Neurosci* 13: 133–140
- McAlister GC, Nusinow DP, Jedrychowski MP, Wuhr M, Huttlin EL, Erickson BK, Rad R, Haas W, Gygi SP (2014) MultiNotch MS3 enables accurate, sensitive, and multiplexed detection of differential expression across cancer cell line proteomes. *Anal Chem* 86: 7150–7158
- Meng XM, Huang XR, Xiao J, Chung AC, Qin W, Chen HY, Lan HY (2012) Disruption of *Smad4* impairs TGF- $\beta$ /Smad3 and Smad7 transcriptional regulation during renal inflammation and fibrosis *in vivo* and *in vitro*. *Kidney Int* 81: 266–279
- Morizane R, Lam AQ, Freedman BS, Kishi S, Valerius MT, Bonventre JV (2015) Nephron organoids derived from human pluripotent stem cells model kidney development and injury. *Nat Biotechnol* 33: 1193–1200
- Mukhopadhyay A, Deplancke B, Walhout AJ, Tissenbaum HA (2008) Chromatin immunoprecipitation (ChIP) coupled to detection by quantitative real-time PCR to study transcription factor binding to DNA in *Caenorhabditis elegans*. *Nat Protoc* 3: 698–709
- Nakagawa S, Nishihara K, Miyata H, Shinke H, Tomita E, Kajiwara M, Matsubara T, Iehara N, Igarashi Y, Yamada H *et al* (2015) Molecular markers of tubulointerstitial fibrosis and tubular cell damage in patients with chronic kidney disease. *PLoS One* 10: e0136994
- de Paz-Lugo P, Lupianez JA, Melendez-Hevia E (2018) High glycine concentration increases collagen synthesis by articular chondrocytes *in vitro*: acute glycine deficiency could be an important cause of osteoarthritis. *Amino Acids* 50: 1357–1365
- Pecot CV, Rupaimoole R, Yang Da, Akbani R, Ivan C, Lu C, Wu S, Han H-D, Shah MY, Rodriguez-Aguayo C *et al* (2013) Tumour angiogenesis regulation by the miR-200 family. *Nat Commun* 4: 2427

- Pereira FA, Qiu Y, Zhou G, Tsai MJ, Tsai SY (1999) The orphan nuclear receptor COUP-TFII is required for angiogenesis and heart development. *Genes Dev* 13: 1037–1049
- Picard N, Baum O, Vogetseder A, Kaissling B, Le Hir M (2008) Origin of renal myofibroblasts in the model of unilateral ureter obstruction in the rat. *Histochem Cell Biol* 130: 141–155
- Pinney DF, Emerson Jr CP (1989) 10T1/2 cells: an *in vitro* model for molecular genetic analysis of mesodermal determination and differentiation. *Environ Health Perspect* 80: 221–227
- Planchais J, Boutant M, Fauveau V, Qing LD, Sabra-Makke L, Bossard P, Vasseur-Cognet M, Pegorier JP (2015) The role of chicken ovalbumin upstream promoter transcription factor II in the regulation of hepatic fatty acid oxidation and gluconeogenesis in newborn mice. *Am J Physiol Endocrinol Metab* 308: E868–E878
- Polvani S, Tarocchi M, Tempesti S, Mello T, Ceni E, Buccoliero F, D'Amico M, Boddi V, Farsi M, Nesi S et al (2014) COUP-TFII in pancreatic adenocarcinoma: clinical implication for patient survival and tumor progression. *Int J Cancer* 134: 1648–1658
- Principe DR, Doll JA, Bauer J, Jung B, Munshi HG, Bartholin L, Pasche B, Lee C, Grippo PJ (2014) TGF-beta: duality of function between tumor prevention and carcinogenesis. *J Natl Cancer Inst* 106: djt369
- Proctor G, Jiang T, Iwahashi M, Wang Z, Li J, Levi M (2006) Regulation of renal fatty acid and cholesterol metabolism, inflammation, and fibrosis in Akita and OVE26 mice with type 1 diabetes. *Diabetes* 55: 2502–2509
- Qin J, Wu SP, Creighton CJ, Dai F, Xie X, Cheng CM, Frolov A, Ayala G, Lin X, Feng XH et al (2013) COUP-TFII inhibits TGF-beta-induced growth barrier to promote prostate tumorigenesis. *Nature* 493: 236–240
- Rabelink TJ, Carmeliet P (2018) Renal metabolism in 2017: Glycolytic adaptation and progression of kidney disease. *Nat Rev Nephrol* 14: 75–76
- Ran FA, Hsu PD, Wright J, Agarwala V, Scott DA, Zhang F (2013) Genome engineering using the CRISPR-Cas9 system. *Nat Protoc* 8: 2281–2308
- Rangarajan S, Kurundkar A, Kurundkar D, Bernard K, Sanders YY, Ding Q, Antony VB, Zhang J, Zmijewski J, Thannickal VJ (2016) Novel mechanisms for the antifibrotic action of nintedanib. *Am J Respir Cell Mol Biol* 54: 51–59
- Rockey DC, Bell PD, Hill JA (2015) Fibrosis—a common pathway to organ injury and failure. *N Engl J Med* 372: 1138–1149
- Romagnani P, Remuzzi G, Glassock R, Levin A, Jager KJ, Tonelli M, Massy Z, Wanner C, Anders HJ (2017) Chronic kidney disease. *Nat Rev Dis Primers* 3: 17088
- Ruas J, White J, Rao R, Kleiner S, Brannan K, Harrison B, Greene N, Wu J, Estall J, Irving B et al (2012) A PGC-1 $\alpha$  isoform induced by resistance training regulates skeletal muscle hypertrophy. *Cell* 151: 1319–1331
- Schlaepfer IR, Joshi M (2020) CPT1A-mediated fat oxidation, mechanisms, and therapeutic potential. *Endocrinology* 161: 1–14
- Subramanian A, Tamayo P, Mootha Vk, Mukherjee S, Ebert BI, Gillette Ma, Paulovich A, Pomeroy Sl, Golub Tr, Lander Es et al (2005) Gene set enrichment analysis: a knowledge-based approach for interpreting genome-wide expression profiles. *Proc Natl Acad Sci USA* 102: 15545–15550
- Takamoto N, You LR, Moses K, Chiang C, Zimmer WE, Schwartz RJ, DeMayo FJ, Tsai MJ, Tsai SY (2005) COUP-TFII is essential for radial and anteroposterior patterning of the stomach. *Development* 132: 2179–2189
- Ting L, Rad R, Gygi SP, Haas W (2011) MS3 eliminates ratio distortion in isobaric multiplexed quantitative proteomics. *Nat Methods* 8: 937–940
- Tomasek JJ, Gabbiani G, Hinz B, Chaponnier C, Brown RA (2002) Myofibroblasts and mechano-regulation of connective tissue remodelling. *Nat Rev Mol Cell Biol* 3: 349–363
- Tran MT, Zsengeller ZK, Berg AH, Khankin EV, Bhasin MK, Kim W, Clish CB, Stillman IE, Karumanchi SA, Rhee EP et al (2016) PGC1alpha drives NAD biosynthesis linking oxidative metabolism to renal protection. *Nature* 531: 528–532
- Wessel D, Flugge UI (1984) A method for the quantitative recovery of protein in dilute solution in the presence of detergents and lipids. *Anal Biochem* 138: 141–143
- Wilson PC, Wu H, Kirita Y, Uchimura K, Ledru N, Rennke HG, Welling PA, Waikar SS, Humphreys BD (2019) The single-cell transcriptomic landscape of early human diabetic nephropathy. *Proc Natl Acad Sci USA* 116: 19619–19625
- Wu S-P, Kao C-Y, Wang L, Creighton CJ, Yang J, Donti TR, Harmancey R, Vasquez HG, Graham BH, Bellen HJ et al (2015) Increased COUP-TFII expression in adult hearts induces mitochondrial dysfunction resulting in heart failure. *Nat Commun* 6: 8245
- Wu H, Kirita Y, Donnelly EL, Humphreys BD (2019) Advantages of single-nucleus over single-cell RNA sequencing of adult kidney: rare cell types and novel cell states revealed in fibrosis. *J Am Soc Nephrol* 30: 23–32
- Wynn TA, Ramalingam TR (2012) Mechanisms of fibrosis: therapeutic translation for fibrotic disease. *Nat Med* 18: 1028–1040
- Xie N, Tan Z, Banerjee S, Cui H, Ge J, Liu RM, Bernard K, Thannickal VJ, Liu G (2015) Glycolytic reprogramming in myofibroblast differentiation and lung fibrosis. *Am J Respir Crit Care Med* 192: 1462–1474
- Xie X, Tsai SY, Tsai MJ (2016) COUP-TFII regulates satellite cell function and muscular dystrophy. *J Clin Invest* 126: 3929–3941
- Yang L, Besschetnova TY, Brooks CR, Shah JV, Bonventre JV (2010) Epithelial cell cycle arrest in G2/M mediates kidney fibrosis after injury. *Nat Med* 16: 535–543. 531p following 143
- Zank DC, Bueno M, Mora AL, Rojas M (2018) Idiopathic pulmonary fibrosis: aging, mitochondrial dysfunction, and cellular bioenergetics. *Front Med (Lausanne)* 5: 10
- Zhang S, Hulver MW, McMillan RP, Cline MA, Gilbert ER (2014) The pivotal role of pyruvate dehydrogenase kinases in metabolic flexibility. *Nutr Metab* 11: 10
- Zhao X, Psarianos P, Ghorraie LS, Yip K, Goldstein D, Gilbert R, Witterick I, Pang H, Hussain A, Lee JH et al (2019) Metabolic regulation of dermal fibroblasts contributes to skin extracellular matrix homeostasis and fibrosis. *Nat Metab* 1: 147–157
- Zhao X, Kwan JYY, Yip K, Liu PP, Liu FF (2020) Targeting metabolic dysregulation for fibrosis therapy. *Nat Rev Drug Discov* 19: 57–75